PAN
POLISH ACADEMY OF SCIENCES

Opto-Electronics Review

journal homepage: http://journals.pan.pl/opelre

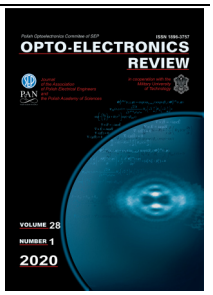

REVIEW

Development of chalcogenide solar cells: Importance of CdS window layer

D. Lilhare[1]* and A. Khare[1]

Thin Film Laboratory, Department of Physics, National Institute of Technology
G E Road, Raipur – 492 010 India

Article info

Article history:
Received 19 Nov. 2019
Received in revised form 31 Jan. 2020
Accepted 03 Mar. 2020

Keywords:
CdS; CdTe; Photovoltaic; window layer; thin films.

Abstract

The solar photovoltaic technology is one of the renewable technologies with the potential to shape a future-proof, reliable, scalable and affordable electricity system. It is important to provide better resources for any upcoming technology. CdS/CdTe thin films have long been considered as one enticing option for reliable and cost-effective solar cells to be developed. N-type CdS as a transparent window layer in heterojunction structures is one of the best choices for CdTe cells. In a solar cell structure, window layer material plays a very crucial role to improve its performance. For this reason, this review focuses on the basic and significant aspects such as importance of the window layer thickness, degradation effect, use of nano-wire arrays, and an ammonia-free process to deposit the window layer. Also, an attempt has been made to analyze various processes improving window layer properties. Necessary discussions have been included to review the impact of solar cell parameters on the above aspects. It is anticipated that this review article will fulfill the requirement of knowledge to be used in the fabrication of CdS/CdTe solar cells.

1. Introduction

Global energy crisis and intemperance in environmental pollution are the foremost essential problems our world is facing. One of the chemical elements, hydrogen is thought to be the foremost enticing potential energy carrier that is ready to resolve these issues within the future because of its renewable and environment-friendly characteristics [1]. In 1972, after photo-electrochemical water ripping for chemical element production on the TiO2, a semiconductor electrode was discovered [2]. The tactic has been additionally applied to the particulate system for finishing up heterogeneous photo-catalysis [3]. However, the sensible application of this technology is restricted by developing a well-designed photocatalyst with each smart stability and activity that nevertheless is a challenge up to now [4].

Demanding seeks for low-cost and clean energy sources have enhanced intensive significance within the progress of solar applications. By using the semiconductor photoelectrode, solar energy directly converts into an electrical energy; this has attracted a lot of researchers for several years. There is an imperative universal requirement for an alternative of renewable energy sources for reciprocally environmental and economic reasons [5–7]. An individual extraordinarily enticing energy resource is the Sun that unceasingly sends immense amount of light energy to the planet's surface [8]. However, harnessing this light energy needs the growth of cheap resources' arrangement capable of harvesting sunlight by expeditiously capturing light energy speedily. Nanotechnology provides new possibilities to attain greater efficiencies of solar power at lower prices. Solar to

Corresponding author: dev17jyoti@gmail.com

https://doi.org/10.24425/opelre.2020.132500

electrical conversion processes have always been a promising and challenging frontier for scientific and technological applications [6,7].

As the world is affected by the imminent loss of fossil fuels and resulting heavy pollution, an alternative energy source is currently thought to be one prominent resolution to the world energy crisis. Among numerous suggestions for producing energy from the Sun, solar cells are a good move towards to convert solar power into sensible voltage. In 2009, the worldwide production of solar cells and modules was of 12.3 GW [9], and one year later, it increased by over 20 GW [10]. Numerous varieties of solar cells based on Si [11], thin film [12,13], and organic materials [14,15] are progressively developed these years. As per the US Department of Energy, solar power ought to solely be economically viable for large-scale production, if the value is reduced to $0.33/Wp (Wp meaning watt peak) [16]. The watt-peak principle is used to measure performances of solar photovoltaic (PV) installations and to estimate the amount of electricity that can be generated under ideal conditions. Solar modules have a watt peak rating. Watt peak (kilowatt peak is often used for PV plants) reflects peak power. This value defines the output power obtained under maximum solar radiation by a solar module (under specified standard test conditions). For describing normal conditions, 1000 watts solar radiation per square meter is used. Fig. 1 illustrates the energy consumption by energy sources.

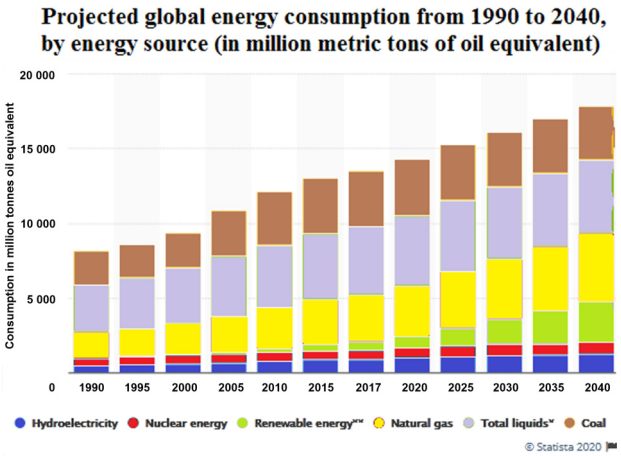

Fig. 1. Energy consumption by fuel (1990-2040). (Source: Statista)

In 1839, the PV effect was discovered; however, it remained of laboratory interest till the middle 1950s once the US space program attempted to power satellite with PV cells. Solar power is one of the feasible power sources in the future for our planet. It is ranked third after hydro and wind in renewable energy. To generate enough power for residential use, solar panels are formed which is constructed by solar modules. One module is constructed through numerous cells connected in parallel. By combining the entire module, a panel can provide DC electric from individual cells.

Single crystal silicon PV cells with 6% efficiency were reported in 1954 at Bell Laboratories. During the first 1970 energy crisis, both private and public sectors became concerned in terrestrial applications of Si-based PV generation of energy and gradually the field of research moved to different PV materials such as InP, GaAs, CuInSe2 and CdTe [17] based solar cells. Throughout the last thirty years, these analyses and growth attempts resulted in enhancement in conversion efficiency from 6% to 17% for $CuInSe_2$ based and the experimental efficiency of CdTe based solar cell has increased from 8% to 22.1%, though the theoretical limit exceeds 24% [18-21].

II–VI semiconductor nanocrystals whose radii are lower than the bulk exciton Bohr radius form an intermediary class of materials between the molecular bulk states of matter. The quantum confinement of the pair of electron hole leads to an increase in the efficient bandgap with decreasing crystallite thickness, offering new ways of tuning optical and photonic properties [22]. Semiconductors of II–VI groups, such as ZnS, CdS, and ZnSe are widely used for the fabrication of solar cells, optical detectors, piezoelectric transducers, light emitting diodes (LED), and transparent UV-protection devices [23-26].

The current high level of analysis and development of the thin-film polycrystalline CdTe/CdS solar cell is driven by the chance of manufacturing PV modules more inexpensively than ever before. The fabrication of thin film solar cells may be a promising approach for terrestrial and space PV devices [27]. Over the past three decades, CdS has been widely investigated for the proficient use within the fabrication of solar cells. It is known as the wider band-gap semiconductors due to their wide applications in optoelectronics, such as nonlinear optics, visible-LEDs, and lasers. CdS thin film is employed as window material in a heterojunction cell due to its high transparency, low resistivity, easy ohmic contact, direct band-gap transition, high electron affinity, and n-type conductivity [27,28]. CdS-based solar cell structure exhibits better optical confinement towards higher efficiencies. CdS window layer absorbs the blue portion of the solar spectrum due to its low bandgap which induces a reduction in solar cell efficiency [26]. Depending on the deposition conditions CdS thin films can be generated with α and β phases. It is understood that α-CdS also develops perpendicular to the substratum with a columnar structure along the c-axis. It means there are no parallel grain boundaries to the junction that would restrict the flow of photogenerated excessive carriers to the grid [29].

With the comparison of all nearest competitors, stability, reasonable conversion efficiency, and accessibility of low-cost deposition techniques attract the usage of CdS. It is found that the CdS is a superior and dominating semiconductor as a window layer material in a solar cell structure. However, it is very toxic in nature and responds badly towards incident radiations of shorter wavelengths [30]. CdTe is a nearly good absorbent material for thin film polycrystalline solar cells as its bandgap (1.45 eV) closely matches the solar spectrum peak. It has a high coefficient of absorption and good electronic properties [31]. Among other second-generation solar cells, CdTe has evidenced itself to be a leading candidate for the development of cost-effective PV devices [32]. The standard radiations received on the earth's surface (AM 1.5) are incredibly wealthy in photons with the energies ranging from 1.4 eV to 3.0 eV [33]. It is already established that in CdTe solar cells, CdS is

popularly used as a window layer which is paired with a p-type CdTe as an n-type heterojunction partner. Since the CdTe and CdS bandgaps are of 1.45 eV and 2.4 eV, respectively, this means that photons with energies < 2.4 eV enter the CdTe layer and contribute to the cell's photocurrent. A significant amount of solar spectrum radiation because of the recombination sites high density in CdS films with wavelength (< 512 nm) is absorbed in CdS and wasted. This loss in photocurrent is nearly 7 mA/cm^2 [34]. Since the absorption coefficients of II-VI compounds are high [35], higher energy photons are absorbed in the window layer leading to the reduction in a light current. Secondly, if the depletion region is much away from the entrance for photons and recombination is significant, this also causes decrement in a light current.

A solar cell has fundamentally major parameters such as the maximum power point (P_{max}), the energy conversion efficiency (η), and the fill factor (FF). P_{max} is a product of the maximum cell current (I_{max}) and the voltage at the max power output of the cell (V_{max}). This point is positioned at the "knee" of the curve.

FF is primarily related to the resistive losses in a solar cell. It is a function of a difference between the I-V characteristics of an actual PV cell and those of an ideal cell. FF is defined as:

$$FF = \frac{I_{max}V_{max}}{I_{sc}V_{oc}}\ , \tag{1}$$

where, I_{sc} (short circuit current) is nothing but the light generated current. It is the maximum current produced by a solar cell when its terminals are shorted and V_{oc} (open circuit voltage) is the maximum voltage that can be obtained from a solar cell when its terminals are left open. The I_{sc} depends on the solar cell area. To remove the reliance of the solar cell region on I_{sc}, the short-circuit current density (J_{sc}) is also used to characterize the maximum current a solar cell produces.

The two resistances mainly affect FF, as well as the efficiency of a solar cell: series' resistance (R_s) and shunt resistance (R_{sh}). Series resistance is the summation of the resistances that come in the current path. It consists of a base, emitter, metal contact resistance and a semiconductor-metal contact resistance. Series' resistance value should be as low as possible. Shunt resistance is because of the current outflow across the p-n junction. The reason behind this may be defects in crystal or impurities' precipitates in the junction region. Shunt resistance value should be as high as possible. An ideal solar cell has an FF of more than 0.80 or close to this. One more important parameter is the conversion efficiency (η) which is defined as a ratio of the maximum power output to the power input to the cell:

$$\eta = \frac{P_{max}}{P_{in}}, \tag{2}$$

where P_{in} is the power input to the cell defined as the total radiant energy incident on the cell's surface.

In this paper, we tried to review the contribution of CdS material as a window layer on the PV performance in different conditions. We included importance of the window layer thickness, impact of degradation uses of nano-wire arrays, and AF process for the window layer in a PV cell. We also tried to focus on the window layer improvement, so that the window layer properties get to enhance and fulfill the solar cell requirement.

2. Solar cell processing different steps using CdS window material

2.1. Reduction in thickness of the CdS window layer

In a critical CdTe/CdS solar cell, the CdS window layer has its own importance. Its thickness needs to be optimized as per requirement. As we know in a short wavelength region, the CdS window layer is associated to the spectral response (SR) and it plays crucial part in deciding the CdTe active layer crystallinity. When radiations fall on a solar cell, not all photons are transmitted by the window layer, but few of them are absorbed by it. This, in turn, affects the cell efficiency. The absorption of photons in the window layer is to be prevented anyhow. Reducing thickness of the PV active layer is the most essential requirement for reducing production costs and harmful influence of Cd toxicity. In a CdS/CdTe thin film solar cell, this is achieved by reducing thickness of the CdS layer. There are several reports where the value of 100 mA/cm^2 of J_{sc} was recorded which is greater than 24 mA/cm^2 [36-38]. In the following paragraphs, we present an analysis of various cell parameters influenced by the CdS layer thickness.

McCandless and Hegedus [39] performed some experiments using different thicknesses of CdS as a window layer. They analyzed the effects of a reduction in thickness of CdS in CdS/CdTe solar cells. They reported a post-deposition process for evaporated CdS/CdTe solar cell structures which was involved in various chemical and heat treatments [40]. Thickness of the CdS film in these devices was taken to be less than 0.2 μm. The values of V_{oc} were found to lay between 0.75 V and 0.778 V, while FF values fell between 70% - 72%, which was quite acceptable for high-efficiency cells. Due to the greater thickness of the CdS layer (1.5 μm), the fabricated devices showed a relatively low J_{sc} value (18-19 mA/cm^2). This prevented photo-generation at wavelengths below the CdS band edge, i.e., 520 nm. In direct bandgap semiconductors like CdS, the photon absorption rate is high and even a thin layer of CdS is capable to absorb a sufficient number of photons. An adequate reduction in the thickness of the CdS layer leads to enhancement in various parameters. The group expected an increase of 4-5 mA/cm^2 in J_{sc} upon reducing the CdS thickness from 1 to 0.1 μm. Though, they tried to increase J_{sc} by changing the thickness (< 0.3 μm) of CdS layers; however, they observed losses in FF and V_{oc} with a minor increase in J_{sc} than expected.

In the variation in thickness of the CdS layer from 0.12 μm to 1.5 μm in CdS/CdTe solar cells, the short circuit SR was analyzed by the authors. Below the CdS band-edge, with a decrease in CdS thickness, the SR increased gradually. The best efficiency was observed for the CdS thicknesses' range between 1.5 μm to 0.03 μm. As the thickness decreases from 1.5 μm to 0.20 μm, the values of V_{oc} and FF observed nearly constant, but no increment was observed in J_{sc}. Conversely, when CdS thickness was below 0.2 μm, the values of V_{oc} and FF decreased considerably whereas, the increment was observed in the value of J_{sc}.

With the thickness of $d \leq 0.24$ μm, the comparison between the current response below the wavelength of 520 nm and the response between wavelengths of 520 nm and 620 nm is explained. As thickness decreased, the collection of current was reported to increase below 520 nm that was partially equalized by the drop in a collection of current between the wavelengths 520 nm and 620 nm (compared with the thickest CdS). With thin CdS films, this response loss between 520 nm and 620 nm (loss in J_{sc} equal to 0.7 mA/cm^2) was not observed to be recoverable with reverse bias (gain in J_{sc} equal to 1.0 mA/cm^2 below 520 nm). It demonstrated that the reduction was due to generation but not due to recombination. Similarly, SR for the long-wavelength edge for the same devices was reported. As the CdS thickness was decreased to 0.12 μm, a shift was reported in the absorption edge of CdTe to lower energies. Thin evaporated CdS films with a thickness of < 0.30 μm were observed to be consisted mostly of small grains of < 0.l μm, whereas > 1.0 μm thick CdS films are reported as columnar structure of grain with ~0.5 μm grain size. In the following processing, due to the small grains, the increment in surface area was observed to be an enhancement of the relations between CdS and CdTe.

Nakamura *et al.* [41] reported the performances of the CdS (as window layer) on CdS/CdTe solar cells with a thickness of 2-μm (1.8 μm $< d_P <$ 2.3 μm). For the deposition of a CdS film, the metal-organic chemical vapor deposition (MOCVD) technique was used. Figure 2 demonstrated the performances of PV as a function of d_{CdS}.

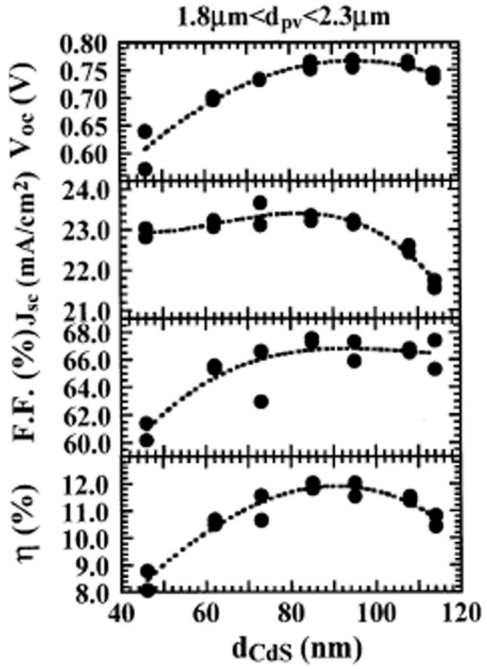

Fig. 2. Performances of PV: d_{CdS} (function of thickness of CdS layer), (A.M. 1.5, 100 mW/cm^2). Reproduced from Ref. 41.

In their study, J_{sc} was found to increase upon reducing the CdS thickness from 114 nm to 95 nm. This was probably due to a blue response of the studied cell. The reduction of d_{CdS} to 95 nm with the increment in the value of J_{sc} is purely concluded through an enhancement in SR at the region of a short wavelength. This increase in SR at the short wavelength region is because of the loss in optical absorption in the CdS layer. For the CdS thickness below 85 nm, the efficiency mostly decreased because of reduction in *FF* and V_{oc}. This suggests that the CdS layer thickness cannot be reduced to any extent and should be of more than the particular value. In the reported paper, the window layer thickness critically influenced the formation of $CdTe_{1-x}S_x$ (mixed-crystal layer) and the CdTe grain development. As a result of a reduction in the configuration (x) of sulfur (S) of a $CdTe_{1-x}S_x$ film, crystallinity deterioration of the CdTe layer was concluded to be the most probable mechanism for the huge decrease in *FF* and V_{oc}. In this way, the CdS layer largely influenced the properties of diode rather than optical properties as the window layer. The diagram of a CdS/CdTe solar cell is shown in Fig. 3.

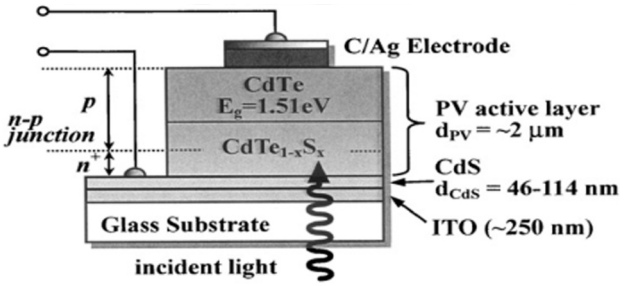

Fig. 3. Schematic diagram of CdS/CdTe solar cell. Reproduced from Ref. 41.

In continuation of a previous work, Kephart *et al.* [42] fabricated CdS/CdTe thin film solar cells using a high-resistance transparent (HRT) layer with Zn stannate and intrinsic tin oxide and reported on various optical losses occurring during the process. As we know that the optical absorption of sunlight photons in a CdS layer is the main cause of loss in CdS/CdTe thin film solar cells. Thickness reduction of a CdS layer under the critical value results in the degradation of device's V_{oc} and *FF*. Presence of a buffer or an HRT layer decreases CdS thickness and V_{oc} value. Thickness and resistivity were maintained at 100 nm and 1-10 cm, respectively. HRT buffer is usually allowed to reduce the parasitic absorption of the window layer (for thinning) and so that the light transmission gets enhanced into the absorber layer and improves the photocurrent. If the HRT layer is not used, then the TCO on glass substrates is normally used with the rough surface resulting in the bad substrate coverage and the creation of the bad junction between the TCO-absorber layers. The extreme window layer thinning often leads to a bad substrate coverage [43,44]. The existence of an HRT layer essentially enhances the excellence of a diode with a CdS thin layer. Thus, buffer or HRT layers were found to extend the efficiency of fabricated CdS/CdTe solar cells. Several TCO and TCO/HRT-coated substrates were tried to fabricate CdS/CdTe cells. Kephart and co-workers varied the thickness of the CdS layer over a range and studied different properties. Below a critical value of CdS, the device performance showed gradual dependence on V_{oc} and *FF*.

Authors made devices in varied CdS thicknesses such as 110 nm, 90 nm, 70 nm, and 40 nm at standard conditions. In this paper also the value of J_{sc} increased with decreasing thickness value of CdS. While CdS thickness was decreased, V_{oc} and *FF* also started to decrease.

With the reduction in CdS thickness, a light-dark intersect was observed to emerge in the devices and became more prominent with the lower V_{oc}. It emerged that the barrier was modulated at the front of the device by light absorption. This intersects' effect was observed to be the most prominent in devices without deposition of CdS where CdTe was deposited directly on the substrate.

With the above discussed attractive properties, improvement in the efficiency of CdS/CdTe thin film solar cells was hindered for decades due to many challenges. One such challenge faced by the PV group worldwide is to manufacture pinhole-free thin films with minimal flaws and maximum concentration of doping. More pinholes mean that all wavelengths are passed and, therefore, similar to larger bandgaps. Because of the creation of pinholes at the junction, the electrical field becomes weaker due to the reduced junction area which improves the recombination of charging carriers. The existence of pinholes can cause a large variation in cell efficiency, as well [45].

The common feature of CdS layers, especially in chemically deposited CdS layers, some pinholes remain after deposition. This may happen due to the formation of small voids that are not densely packed between the grains. To get rid of the negative aspects of these pinholes in an n-type window layer in a CdTe solar cell, the CdS layer needs to be very thin and chemically robust to prevent current shunting paths and pinholes from being formed [46].

Impact of the fractional pinhole area was theoretically studied by Kephart *et al*. [42]. They found that pinholes with thinner CdS did not dominate device's performance. Results of their modelling on a CdTe/CdS solar cell indicated that the buffer layer's ohmic behavior had a comparatively little impact on devices with pinholes, in spite of developing the areas of diode with thin CdS layers or without CdS, had a dominant impact.

2.2. *Degradation on CdTe/CdS solar cell parameters*

As the solar energy generation is receiving so much importance worldwide, numerous solar panels are being consecutively interconnected. As a result, solar panels are often exposed to high relative potentials towards the ground causing high voltage stress (HVS). In 2005, NREL addressed the impact of HVS on durable solar panels' steadiness depending on the leakage current between ground and solar cells. They reported that solar modules can degrade due to the inevitable elements like damp heat, thermal cycling, UV exposure, and humidity. So, an average solar degradation rate of 0.8% per year is reported. Gradual degradation in the performance of modules can be a reason for an increase in shunt resistance (R_{Sh}) due to a decreased adherence of contacts or corrosion of the materials.

Crystalline silicon semiconductor is manufactured through the process of silicon purification, wafer slicing, ingot processing, doping and etching which eventually forms a p-n-p junction. Crystalline silicon solar cells do not easily degrade [47,48]. The solar modules combined without moving elements are extremely powerful. Though, modules appear to demonstrate some degradation over time. Degradation can be different from cell to cell, a module to module, etc. Therefore, it is suggested to have fewer degrading modules than that of the non-degrading ones. The proper packaging of modules can also affect cell performance; however, some degradation of the conductor cannot be excluded [49-51].

Mendoza-Perez *et al*. [52] reported degradation effects in CdTe/CdS solar cells. The authors studied the progress of the PV cell parameters like photocurrent and photocurrent density over 3 years. In their study, the CdS layer as a window layer was deposited through chemical bath deposition (CBD) technique with varied S/Cd ratios. Shunting effects were observed to weaken/degrade cell performance, especially *FF*. In order to obtain a long steady CdTe/CdS PV cell, it was concluded to avoid metal inside the back contact [53]. Grain boundaries provided sensible diffusion paths and accelerated cell degradation by shunting. Grain boundaries have been found primarily by providing additional recombination sites inside the semiconductor material to reduce the performance of polycrystalline solar cells. Still, Cu remained the choice as a back contact in model cells. This group of authors pointed out that a contact diode is formed in reverses direction; it may cause a dubious change within the J_{sc} and voltage and limit the PV cell performance. In a solar cell, the use of a chemically deposited CdS layer with nominal ratios (S/Cd=5:1, 6:1 and 7:1) demonstrated lower mean roughness and higher coverage of substrate. The cell parameters measured with different S/Cd ratios for 36 months are enlisted in Table 1. Besides the back contact, changes in the interface of CdTe/CdS also played a crucial role. It may be noted that to minimize the electron-hole recombination, the cell must have a well ordered CdTe/CdS interface. Upon exposing the solar cells/modules/panels to

Table 1
The values of current density (J_{sc}), open circuit voltage (V_{oc}), fill factor (*FF*), efficiency (η), and degradation percentage over a measurement period of 36 months. Reproduced from Ref. 52.

S/Cd	V_{oc}(V) Oct 03-Dec06	J_{sc}(mA/cm^2) Oct 03-Dec06	*FF* Oct 03-Dec06	η (%) Oct 03-Dec06	Degradation (%)
3:1	0.613-0.528	18.7-10.2	0.58-0.33	6.7-1.9	70
4:1	0.74-0.623	18.7-10.9	0.70-0.62	9.8-4.3	55
5:1	0.745-0.649	21.4-17.0	0.70-0.46	11.1-5.4	51
6:1	0.746-0.64	20.2-16.4	0.73-0.57	11.0-6.0	44
7:1	0.73-0.649	18.4-17.6	0.62-0.60	8.4-7.0	17
8:1	0.524-0.450	18.4-5.7	0.57-0.41	5.5-1.1	80

Table 2
The values of series resistance (R_s), parallel resistance (R_p), current density (J_{sc}), fill factor (FF), open circuit voltage (V_{oc}), and efficiency (η): for fabrication of a solar cell using CdS films deposited from bath with nominal ratio S/Cd= 5:1. Reproduced from Ref. 52.

S/Cd=5:1	R_s(Ω cm^2)	R_p(Ω cm^2)	V_{oc}(V)	J_{sc}(mA/cm^2)	FF	η(%)
October 2003	4.8	926	0.745	21.4	0.70	11.1
December 2003	6.0	1080	0.716	21.3	0.64	9.7
June 2004	8.5	832	0.720	20.2	0.63	9.2
December 2004	18.8	912	0.740	22.0	0.51	8.4
December 2005	49.0	217	0.707	21.5	0.45	6.8
December 2006	108	309	0.649	17.0	0.46	5.4

outside conditions, it faces deterioration and oxidation of component semiconductor materials and back metal contacts employed in the PV cell.

Due to changes in R_s, the reduction in FF with time (Table 2) could be associated with chemical changes. Authors had estimated that in samples with massive grains a quicker chemical reaction method will manifest itself. This could be in the sample with S/Cd = 3:1 and 8:1 ratio. In the graph between J_{sc} and voltage (Fig. 4), J_{sc} was found to saturate after a certain period. This saturation feature of J_{sc} with increasing voltage was primarily associated with a short circuit between Cu–Au metallic contacts and an SnO_2:F film. The Cu segregated through the grain boundary of CdTe and CdS caused a reduction of around 50% within the efficiency. Another reason for the deterioration in PV parameters was native environmental conditions which influenced the overall efficiency [54].

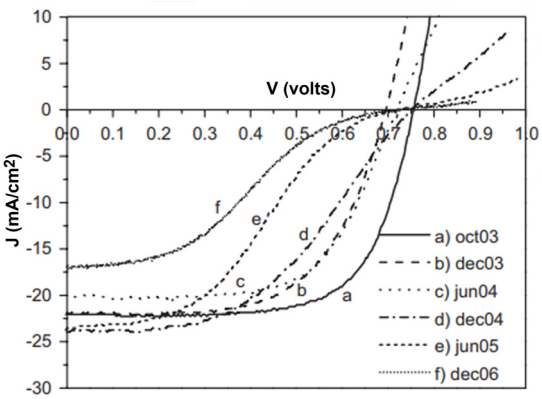

Fig. 4. J vs. V curves (under AM1.5 illumination) during the 36 months period in the case of CdS film deposited from bath with S/Cd ¼ 5:1. Reproduced from Ref. 52.

It is renowned that under solar illumination, CdTe solar cells are often degraded. Other than there is no proof of the degradation mechanism due to its consistent appearance. Ahn et al. [55] investigated CdS/CdTe solar cells' degradation with the lacking Cd composition in a CdTe layer. In this work, the concentration of Cd vacancy is high and reported that the Cu atoms used as a back contact simply filled the vacancies of Cd in CdTe layer and moved to the back contact. Preparation of the rear contact was a challenging task for the Authors in the progress of CdTe solar cells. With the reason of the high electron affinity of CdTe, applying Cu within the back contact had demonstrated to perform the best efficiency. An atom or molecule's electron affinity is the amount of energy released or expended in the gaseous state when an electron is applied to a neutral atom or molecule to form a negative ion. However, on the other hand, the Cu diffused into the CdS layer and caused its degradation. This is the reason for an enormous availability of literature on the rear contact preparation and copper diffusion [56-58]. To stay away from cells' degradation and get efficiency reliable and reproducible, the diffusion of Cu (from back contact) into the window layer (CdS layer) should be controlled. Most of the analyses on degradation problems have been primarily focused.

Three conditions were followed by the Authors: (i) initial (ii) aged and (iii) reverse biased. PL spectra of the CdS layer, at RT (room temperature) were reported. All the peaks showed the emission as required by the conditions of the film as shown in Fig. 5. But the Author's interest factor was on another PL peak which was very sharp and strong observed at 1.55 eV. Since, after the aging process of Cu accretion is well known, Authors made probability that peaks were created due to the occupancy of Cu in the vacancy site of Cd (CuCd). The reported narrow peak was observed by the electronic transition from the conduction band (CB) to CuCd defects. Authors observed that the peak was conspicuous because of the rapid influx of Cu from the back contact while Cd was lacking in CdTe. It was also observed that the peak at 1.55 eV was completely vanished by the third case (reverse-biased stress). These results concluded that Cu atoms were built up in the layer of CdS and they occupied the Cd vacancy sites with the energy peak of 1.55 eV (803 nm) by thermal stress. Authors concluded that the integration of Cu into CdS changed CdS from n-type to less n-type which results as creating in a smaller junction potential.

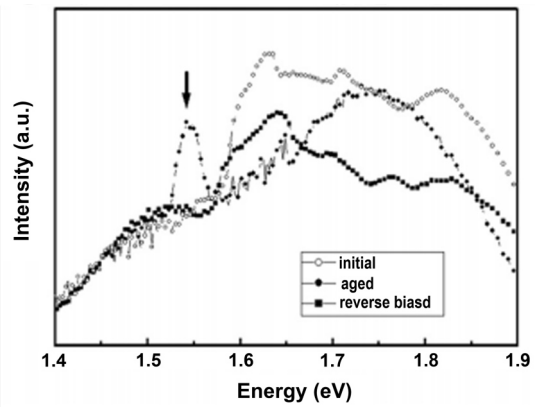

Fig. 5. PL spectra of CdS layers in CdTe cells with initial, stressed (aging), and reverse biased conditions. Reproduced from Ref. 55.

Figure 6 showed the J-V curves of the CdS/CdTe thin film solar cell. The observation was done under three conditions: (i) initial (ii) aged at the temperature of 100 °C for the duration of 10 days in N2 and (iii) reverse-biased at a voltage of 4 V for a duration of 2 hours. In the first condition, the observed values of parameters were as reported: η = 12%, Voc = 0.82 V, Jsc = 21.5 mA and FF = 0.68 and conversely, the parameters were considerably decreased in the second condition, η = 6%, Voc = 0.76 V, Jsc = 17.0 mA and FF = 0.46. Due to the Cu incorporation into CdS observed that the CdS was less n-type and decreased in the potential junction. While applied in reverse bias, the η was increased to 9.5% and the observed value of remaining parameters was of Voc = 0.82 V, Jsc = 17.3 mA, and FF = 0.67 on the thermally stressed cell.

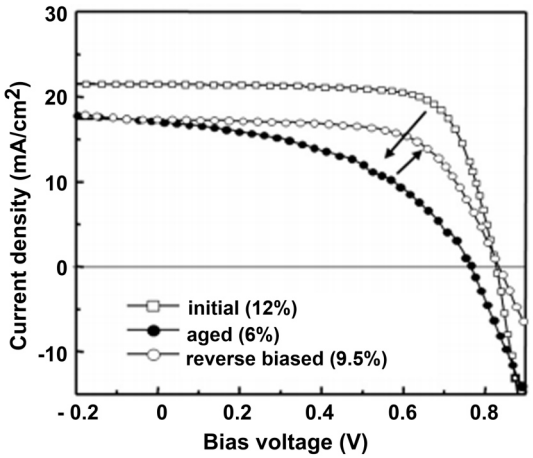

Fig. 6. J-V curves of CdS/CdTe/Cu_2Te/Au cells with initial, stressed, and reverse biased conditions under AM1.5 illumination. Reproduced from Ref. 55.

Similar results were also shown in schematic band diagrams [Fig. 7(a)] of CdS/CdTe thin film solar cells: before stress and after stress. When CdS was n-type, the junction built-in potential was large in both stress tests, but when the CdS was less n-type because of the Cu integration resulted, the junction built-in potential small $\varphi_2 < \varphi_1$ as shown in Fig. 7(b).

Authors also reported the study of spectral quantum efficiency and observed the transfer of electrons from the level of the Cu acceptor to the CB. Only a part of the incident light traveled through the CdS layer upon shielding the incident light (> 1.55 eV). It concluded that the light generated current and V_{oc} were so low that changed the light penetration and the potential for junction resulted in degradation of the cell performance. To keep away from this degradation and get a reliable and reproducible performance, the CdS layer should be controlled from the Cu diffusion from the back contact. Authors also suggested the following aspects from keeping away the degradation: CdTe composition should be stochiometry and in case of any probability of CdTe vacancy defect must be suppressed.

As it is known CdTe has a high work function of 5.7 eV and it is not possible to comprehend the ohmic contact to a

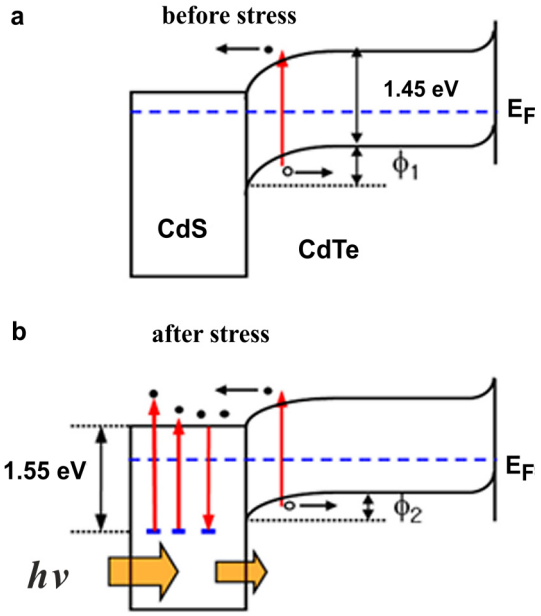

Fig. 7. Schematics of energy band diagram of CdS/CdTe solar cells with (a) before and (b) after stress test. Reproduced from Ref. 55.

p-type CdTe partially. The work function of CdTe is larger than of other common metals. The maximum efficient CdTe cells were formed with Cu comprising back contact by using Cu_xTe [59]. Though, due to the Cu diffusion, there is a critical issue on the stability of Cu-containing contacts. To overcome the stability issues, Lin *et al.* [60] investigated some Cu-free back contact buffer layer material so that it would be easy to optimize the new type of material as a back contact which can overcome the problem regarding cell performance and stability. To improve the ohmic contact between indium-tin-oxide (ITO) and the transition metal oxides such as molybdenum oxide (MoO_x), vanadium oxide, nickel oxide, and tungsten oxide have been used as an anode buffer layer material. Especially, as reported in some literature, MoO_x has an extraordinarily high work function of 6.80 eV – 6.86 eV and has a quality of being easy to prepare by vapor deposition technique [61,62]. MoO_x was observed as a very beneficial buffer layer (low-resistance back contact) instead of the solution etching treatment technique According to the Authors, the removal of surface residues from the CdTe surface is necessary, as well as the use of the thermal evaporation technique deposited on a MoO_x film to establish ohmic contact.

Several metals with a MoO_x film (buffer layer) were used as a back electrode. MoO_x has the best quality providing an instant contact with such type of materials like CdTe. Different metals such as Mg, Al, Ni, Cr and Mo were used as electrodes. Characterization of J-V curve of CdTe solar cells with MoO_x and numerous metal electrodes are shown in Fig. 8. Table 3 illustrated a description of the performance of device parameters including metals work functions. The cell efficiencies from 11.5% to 12.9% were observed.

Table 3
Properties of metals applied to CdTe/MoOx films and the associated device performance parameters. The properties include work function (Φ_m), possible metal oxides (M_xO_y) and standard enthalpy of formation of the metal oxides. Reproduced from Ref. 60.

Metal	Φ_m(eV)	M_xO_y: Standard enthalpy of formation (kJ/mol)	J_{sc} (mA/cm^2)	V_{oc}(mV)	FF (%)	η (%)
Ni	5.04-5.35	Ni_2O_3: -489.5	22.0	808	72.6	12.9
Mo	4.36-4.95	MoO_3: -745.1	21.9	817	68.1	12.2
Cr	4.5	Cr_2O_3: -1139.7	22.0	805	65.0	11.5
Al	4.06-4.26	Al_2O_3: -1675.7	22.3	815	68.4	12.4
Mg	3.66		21.7	811	71.9	12.7

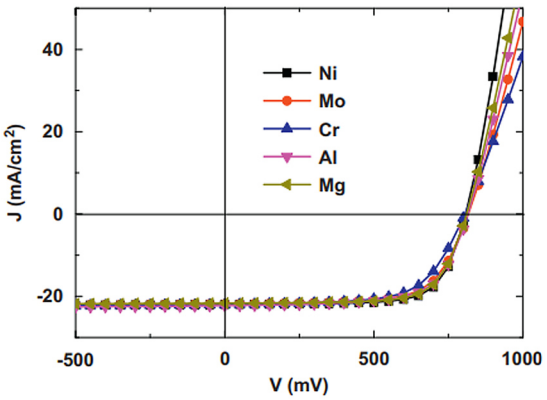

Fig. 8. J–V characteristics of CdTe cells with a MoOx buffer layer and with variousmetal electrodes: Ni, Mo, Cr, Al and Mg. Reproduced from Ref. 60.

Authors also studied thermal stability of the cells with different metals. They annealed the cell at 200 °C in a vacuum. During 19 h of the annealing process, the changes in the cell performance parameter were observed by the Authors (Fig. 9). The cell degradation rate was emerged in the first 4.5 h, after that no change was recorded, the rate was observed approximately equaling zero. The cells with electrodes such as Mo (16.9%) and Ni (13.5%) were the most stable. Conversely, the cell with Al electrode was stated to be the least stable and showed a 63.2% degradation including a huge enhancement in series resistance. It concluded that the cell degradation is always linked with a roll-over behavior improvement.

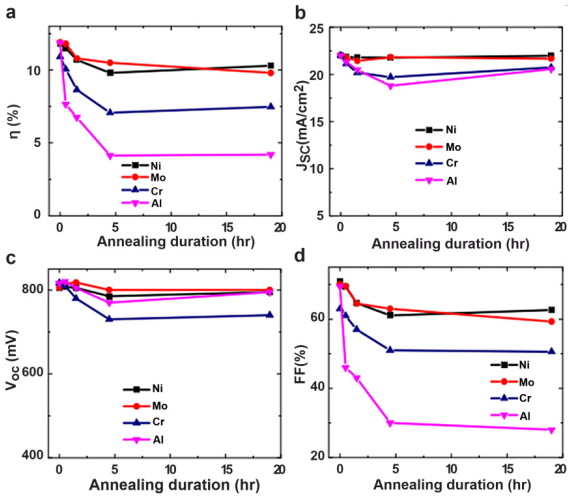

Fig. 9. Evolution of cell performance parameters during the thermal annealing test: (a) *η*, (b) J_{sc}, (c) V_{oc}, and (d) *FF*. Reproduced from Ref. 60.

2.3. *Nano-wire arrays for window layer applications*

Over the last few decades, solar cell devices have been developed progressively and found an efficient way for conversion of sunlight into electricity [63,64]. Especially, Si [65], CdTe [66–69] and CIGS [70] have arisen as the major absorber semiconductors in solar cells. Though, for the last ten years, the development of light conversion efficiency of CIGS and CdTe based solar cells has been comparatively small in comparison with Si-based solar cells [71]. Due to this, optimization of the fabrication process is becoming saturated. An appreciable number of researchers are trying to explore new designs that could further improve the solar to electric conversion efficiency involving nanostructured materials [72,73]. There are published several reports exhibiting the advantages of the nanostructured cell design over bulk films [74,75]. Nanotechnology can prove to be the most auspicious field with high proficiency and less cost for the next generation solar cells. Since the nanostructures are smaller than standard designs for solar cells, there is a possibility to achieve greater efficiency employing nanostructured designs. Since the novel technology is growing up and the perceptive of size effects becomes deeper, nanotechnology is estimated to exceed the latter by wide margins.

As a result of their unique and interesting properties and applications superior to their bulk counterparts, nanostructures have received a progressively increasing interest (with dimension between 1 and 100 nm) [76]. These nanostructures are solids which exhibit a distinct variation in optical and electronic properties with a variety of particle size less than 100 nm. These nanostructures are categorized as one dimensional (1D) or quantum wires, two dimensional (2D) or quantum well and zero-dimensional (0D) or quantum dots. They are capable to find many important technological applications and displaying novel electro-optical, chemical, structural and magnetic properties [77].

1D semiconductor nanostructures such as nano-rods, nano-tubes, nano-belts and nano-wires (NWs) have recently received significant interest due to their distinctive optical, electronic, mechanical properties and their potential applications in the fabrication of nanodevices [78–80]. 2D nanostructures (thin film) [81] have been broadly studied by the semiconductor community because they are convenient to prepare using techniques such as molecular beam epitaxy (MBE) [82]. In the past two decades major improvement has been made with regard to 0D nanostructures, as well [83]. For producing quantum

dots, varieties of chemical methods have been developed with well-controlled dimensions and from a wide range of materials [84].

In PV devices, the nanostructures of CdS films were applied to form the hetero junction with bulk CdTe layers. Nanostructured CdS can be synthesized in the form of crystalline, porous and fibers. These CdS structures are made from different processing procedures but possess similar structures of thin film solar cells. For realization of various nano-scale techniques, variety of experimental approaches have been developed, such as film deposition by means of sputtering, E-beam evaporation and closed-space sublimation (CSS), and crystal growth methods of direct current (DC) electrochemical [85] deposition in template synthesis, catalytic chemical vapor deposition (CVD) growth [86]. To fabricate the nanocrystalline CdS films, solution growth, chemical and microwave-assisted synthesis are preferred. Nano-porous CdS films are fabricated from the ultrasound irradiation which forms nano-fibers/nano-tubes/NWs, which may be created from a mixture of ultrasound and chemistry solution deposition [87].

In nanoscale devices, due to their innovative basic potential applications and properties, NWs have drawn considerable experimental and theoretical interest [88-91]. The II-VI binary semiconductor NWs acquire distinctive optical and electronic properties. These NWs are useful in popular nanoscale devices such as LEDs, [92,93] single-electron transistors, [94], and thin-film field-effect transistors [95]. The properties of semiconductor NWs are highly size-dependent, [96] and so accurate in controlling their size, such as the aspect ratio (length/diameter) and diameter. For optoelectronic and electronic applications, the energy bandgap of binary semiconductor nanostructures is an essential parameter.

The typical structure of a solar cell with CdS NW films is shown in Fig. 10. The sunlight directly falls on glass substrates and photons are absorbed by n-type CdS nano-fibers and p- type CdTe layer. The electrochemical synthesis [97] has been considered as one of the most efficient methods to control the growth of CdS NWs. The generation of CdS NWs is controlled by choosing different values of current and time durations. Deposited CdS NWs were perfectly mounted in the direction perpendicular to the substrate surface.

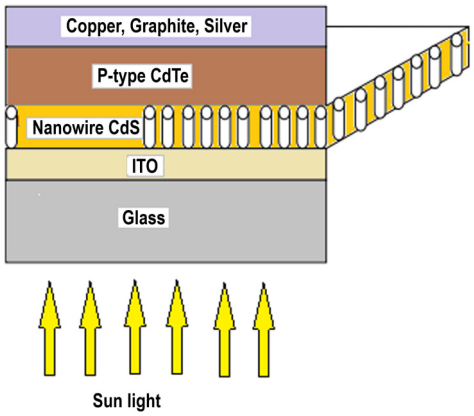

Fig. 10. Structure of CdS nano-wire solar cell.

It is observed by the researchers of Electronic Device Research Lab (EDRL) that the CdS NW layer has a higher transmittance than the conventional planar CdS layer (window layer). They found that the absorption peak of CdS NWs had shifted slightly from 512 nm (for conventional CdS solar cells) to 480 nm (for CdS NW solar cells) towards the sunlight blue region [98]. As a result, more photons are absorbed by the CdTe layer and the produced light current is increased.

As an alternative to thin CdTe and CdS films, CdTe and CdS NWs arrays are being studied. In the absorber semiconductor, the wire array scan provides more effective photon absorption and is more efficient in carrier collection, as well [99–102]. In order to reach greater light conversion efficiencies, the CdS NWs arrays need to pass an enormous number of photons that can enter the absorber layer and convert it to charge carriers there. Previously, Guduru *et al*. [98] reported about the Schottky diodes on CdS NWs. In their work, they observed that the CdS NWs' length was much higher than 100 nm. Therefore, CdS NWs were found unsuitable in solar cells as a window layer like CdS/CIGS and CdS/CdTe. 3DWorking on the same line, Fan *et al*. [101] developed n-type CdS nano-pillars (3D). These pillars were entrenched in a p-type CdTe where they were enabled for an efficient carrier collection. The geometries of a p–n junction cell were developed by the vapor-liquid-solid (VLS) method. The VLS technique is a mechanism from chemical vapor deposition for the development of a 1D structure, such as NWs. The crystal growth on to a solid surface by direct adsorption of a gas phase is usually very slow. The mechanism of VLS circumvents the crystal growth by initiating a phase of catalytic liquid alloy that can speedily adsorb a vapor to the supersaturating level. So, a crystal growth can take place from nucleated seeds at the interface of liquid-solid [103]. In this paper also the length of n-CdS nano-pillars (~1 μm) was rather long. This nano-pillar length will result in a significant loss of the photocurrent because of the light absorption.

Dang *et al*. [104] reported on CdS NW arrays as window layer in solar cells. Authors used the 100 nm long n-type CdS NWs' arrays as a substitute of the planar n-type CdS films. These NWs are presently being used in many solar cell devices for window layer applications. These window layers exhibit the best features of transmittance. They found out that for photon wavelengths greater than 500 nm, the spectral transmission of CdS NW and planar CdS was nearly equal. For a NW layer, the gain in transmittivity took place at wavelengths which were shorter than 500 nm that indicated the strong transmittivity. The transmission of CdS NWs was embedded mainly in the most impactful bandgap energy. The prolonged optical path was not as influential as a consideration for the NW configuration while the improved value of the bandgap energy resulted in more transmitted photons. Authors demonstrated some larger advantages in a transmission of the device configuration of NW over CdS film by a photon flux simulation under the worldwide title AM 1.5D spectrum (Fig. 11).

Authors found out that CdS NW arrays (window layer) yielded higher J_{sc} than a CdS thin film cell. They believed that each additional photon contributed to an additional electron that was captured by the ITO electrode. J_{sc} demonstrated a 5.49 mA/cm^2 rate. This was a 20.6% improvement over the current, 26.6 mA/cm^2 "planar" value.

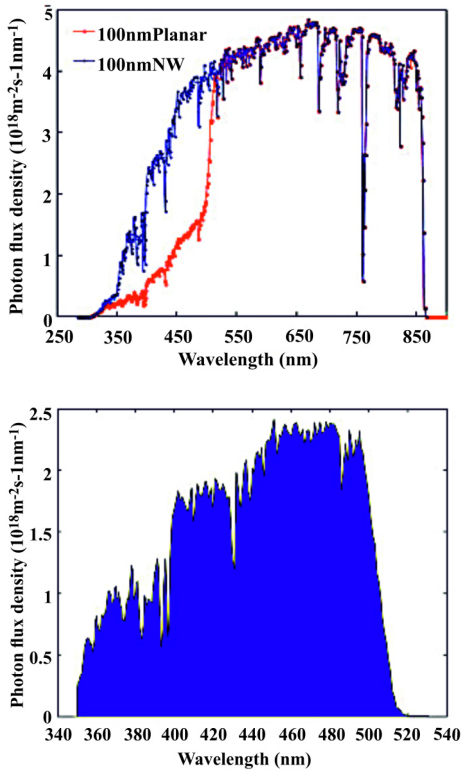

Fig. 11. Comparison of photon flux densities transmitted through a 100 nm long CdS nano-wire array and through a planar CdS film of equal thicknesses. (a) transmitted photon flux densities (b) difference between two photon flux densities. Reproduced from Ref. 104.

Liu *et al*. [105] also reported on CdS NWs as window layer in CdS/CdTe thin film solar cells. CdS/CdTe thin film device is a leading technology for the next generation solar cells. Authors influenced by the Javey group who showed that the CdS nano-pillar arrays had far less reflection of light than a planar film [101]. They designed a 3D complex of CdS and CdTe and created nano-pillar arrays of CdS solar cells. They explained that CdTe NWs interpenetrated and demonstrated a 6% efficiency for cell power conversion [106]. This cell demonstrated the best power conversion efficiency amongst all solar cells-based nano-pillars, NWs, nano-dots, and nano-rods. In order to reach greater power conversion efficiency of solar cell applications, Authors attempted to improve nanomaterials and device configurations.

Two new CdS/CdTe solar cells device configurations are reported by the Authors. The typical CdS window layer in these solar cells was replaced by CdS NWs and entrenched in an anodic aluminum oxide (AAO) matrix. In the device configuration, a growing CdS NW embedded in a nanoporous AAO film. It was built over the transparent electrode as a template. When the transparent AAO template was made from an aluminum foil, an opaque sheet of aluminum adjoined the CdS layer. In that case, sunlight entered through the CdTe side and was thus partially blocked by gold and copper contacts. Therefore, around 50% of incoming light was lost [106]. The sunlight transmitted via the CdS layer when the AAO template was constructed directly over a transparent electrode. No major transmission losses were reported. This was similar operationally to the conventional CdS/CdTe solar cell device front-wall configuration [107] which had the beneficial aspect of absorbing most sunlight close to the p–n heterojunction.

The NW-CdS layer is well known to have larger transmittivity than the conventional CdS layer. As compared to bulk CdS, the absorption peak of CdS NWs was stated to shift towards the blue region [98,108]. Authors reported that the optical absorption edge dropped at 480 nm in CdS NWs [98] rather than 512 nm for the conventional CdS thin film. This effect has shown an increase in the quantity of sunlight photons that have occurred on the CdTe absorption layer and an enhancement in the light-generated current resulting in an enhancement in the efficiency of solar cell. Furthermore, since CdS NWs occupied only a portion that relied on the permeability of the AAO template layer (as window layer) and AAO was observed as an insulator with much greater optical transmittivity. The total transparency improved further and the CdTe layer absorbed more photons.

Liu *et al*. [105] compared the properties of silicon NW arrays and CdS NW, as well. Few reports on such comparisons have been already published [109,110-112]. The study indicated that Si NW arrays had greater absorption than an equally thick planar Si film. This was due to the reflections on the concealed surface [101,112]. The prolonged optical path was induced basically by the dispersion of photons and numerous nanostructures in the matrix of NW. Remarkably, CdS exhibited proficient absorption in the 300 nm – 510 nm range. Conversely, Si is an indirect bandgap material with low absorption coefficient. Hence, in CdS, improved absorption caused by enhanced optical scattering might not be as an essential factor as in the case of Si. It was therefore concluded that CdS NW had higher aluminum oxide transmittivity and reduced edge of absorption which dominated the optical scattering effect.

2.4. Ammonia-free process for solar cells' window layers

It is well known that polycrystalline CdS thin films are widely popular as window material in several heterojunction solar cells, such as CdS/CdTe for their favorable optical properties [113,114]. Recently, there have been so many reports on the application of CdS as a window layer in CdS/CuInSe$_2$, CdS/CdTe and CdS/Cu(InGa)Se$_2$ [115–118] high-efficiency solar cells. To develop the technology for various PV systems, the production cost is the most important factor; it involves energy consumption, as well as resource and development costs in various technological processes. An additional essential aspect is the maintenance of environmental balance. The device production needs to be supported by clean energy and clean technology [119]. Many aqueous methods, such as spray pyrolysis [120], successive ionic

layer adsorption and reaction (SILAR) [121], and CBD are generally preferred for the deposition of the above-discussed CdS films [122–124]. CBD is the simplest, most economical and low-temperature process for a large-scale film deposition among those processes. CBD has been used for the deposition of thin films of chalcogenide semiconductors for many decades [125]. Since the beginning of the 1990s, renewed interest in the CBD CdS films came from the impressive results achieved using them as window layers in thin film solar cells, such as CdTe and $CuInSe_2$ [126]. Besides, such films are made up of tightly packed nanocrystals (NCs) [127] that make them desirable for basic and applied NC research The phenomenon that makes NCs so unique is the quantum confinement effect (QCE) which contributes to the blue change in energy bandgap and is used to spectrally modify semiconductor optical properties [128]. Though, the significant amount of Cd toxic residues is a drawback in applying the CBD procedure in a large area [129]. Even though CBD is somewhat less dangerous, it is recommended that researchers use a fume hood and deposit the films using non-toxic complexing agents. The deposition of CdS thin films by CBD is mainly based on the utilization of ammonia as a complexing agent for Cd ions [128]. Usually, the CBD process for deposition of CdS films is based on a slow release of Cd^{2+} and S^{2-} ions in an aqueous alkaline bath and their deposition on the substrates. In general, ammonia is used to adjust the pH value of the reaction solution [130].

Ammonia is a substance that is highly unpredictable and presents health and environmental risks as it is corrosive to the skin, internal organs, machinery and equipment. Consequently, after the CBD process, the wastewater containing ammonia becomes a serious problem. For ecological safety and lower manufacturing cost, every CBD residue needs to be destroyed [131]. In the CBD process, many approaches were suggested for reducing these undesirable effects. One of these techniques is to recycle and reuse the resulting waste Cd material [132,133]. The other is called ammonia-free (AF) CBD process optimization. Ammonia or ammonia compounds may be replaced in these approaches by other complexing agents such as triethanolamine, ethylenediamine, sodium citrate, ethanolamine [134,135], and nitrilotriacetic acid [128,136]. In aqueous solutions, CdS nanoparticles have been obtained from Cd complexes with amino acids (AAs) [137,138]. In the CBD process, glycine was primarily used as a complexing agent for the preparation of CdS films [139,140]. However, such methods use buffer solutions with ammonia compounds (NH_4OH and NH_4Cl) [141].

Ochoa-Landin *et al.* [135] reported chemically deposited CdS films prepared by an AF process for solar cell window layers. One of the key methods is to remove ammonia as the complexing agent. In the reaction solution, several substances succeeded for removing ammonia for the CdS thin film deposition. In this paper, sodium citrate was used as a substitute for the ammonia. Particularly, sodium citrate is an inexpensive and non-hazardous organic compound, and is extremely suitable for chemically deposition of CdS films. Ammonia is commonly used in the food industry as a flavoring or food preservative and as a popular ingredient in several beverages. Previously published papers [142-145] highlight that the highly crystalline CdS thin films with good uniformity and robustness were achieved by such processes.

Ochoa-Landin *et al.* [135] examined the properties of AF CBD–CdS films deposited on two conductive substrates SnO_2:F (FTO) and In_2O_3:Sn (ITO) and applied them for making the CdS/CdTe solar cell materials. Authors analyzed the properties of CBD–CdS films grown with three types on an ITO and FTO substrates (transparent electrodes). In their work, to deposit the CdS layers, they used the CBD process where ammonia was replaced with sodium citrate as a complexing agent (fully or partly). The three types of CBD-CdS films which included complexing agents as 1) CdS X films which had partial $Na_3C_6H_5O_7$ (sodium citrate), NH_4OH (ammonium hydroxide), 2) CdS Y films which were substituted $Na_3C_6H_5O_7$, KOH (potassium hydroxide) with a pH 10 borate buffer, and 3) CdS Z films contained the similar precursors as in the CdS Y films, with the exception of the pH 10 borate buffer. The authors found that there was an impressive performance in the window layers by using sodium citrate in CBD processes.

The optical transmittance spectra of CdS films deposited on two substrates: ITO and FTO and respective transmission spectra are shown in Fig. 12. The average optical transmissions were obtained to be in the range of 500 nm - 840 nm for both ITO and FTO substrates. The FTO substrates optical transmission displayed lower values in the spectral region than those of the ITO substrates. In the case of higher optical transmission, the energy bandgap values of films deposited on ITO substrates had higher

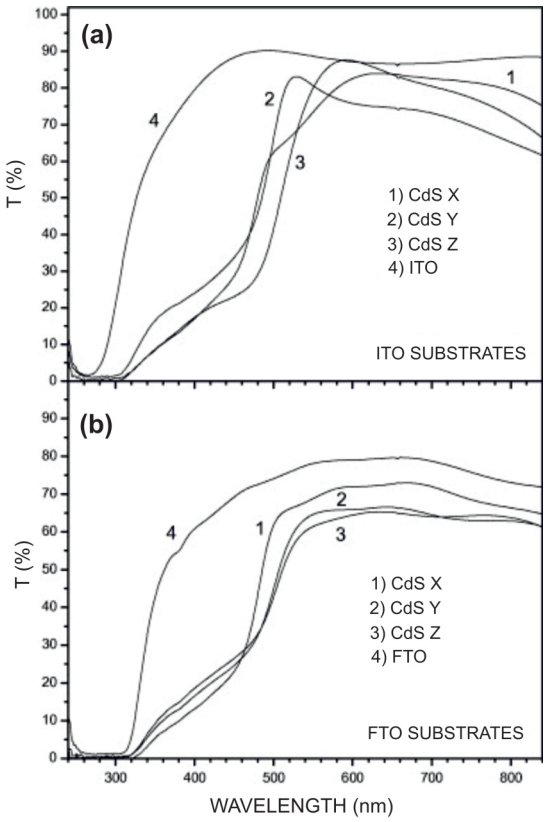

Fig. 12. Optical transmission spectra of X, Y and Z CdS films deposited on (a) ITO and (b) FTO conductive glass substrates. The spectra of ITO and FTO bare substrates were included for comparison in both graphs. Reproduced from Ref. 135.

values than the FTO substrates, which meant a broader range for solar cell absorption layer incident radiation. The broader energy band distribution of CdS films on the ITO substrate was associated with the constant crystalline lattice [146].

Authors also determined the J–V characteristics of CdS/CdTe thin film solar cells under the elucidation conditions of 50 mW/cm^2 (Fig. 13). The J_{sc} and V_{oc} values were achieved of 11.9 mA/cm^2 and 570 – 630 mV range, respectively. The respective *FF* values with relatively low values of final conversion efficiency were between 50% and 58%. Thus, it was concluded that the solar cells fabricated with the same type of chemically deposited CdS films exhibited better performance with ITO/glass as compared to FTO/glass. Thus, citrate-based CB deposited CdS films have been shown to be appropriate for window layer applications. Cell efficiency relied on the front transparent electrode. In the cells, ammonia and sodium citrate employed as the complexing agents, the higher efficiencies were achieved with the window layers of X-CdS. Because of partial replacement of sodium citrate, this method also offered some ecological advantage due to reduction of ammonia. Furthermore, the quantity of Cd was lowered to 0.56 mg/ml in the Y-CdS and Z-CdS window layers. While Y-CdS and Z-CdS performed with lesser efficiency in CdS/CdTe solar cells, both AF processes were found to be very appropriate for the window layers deposition.

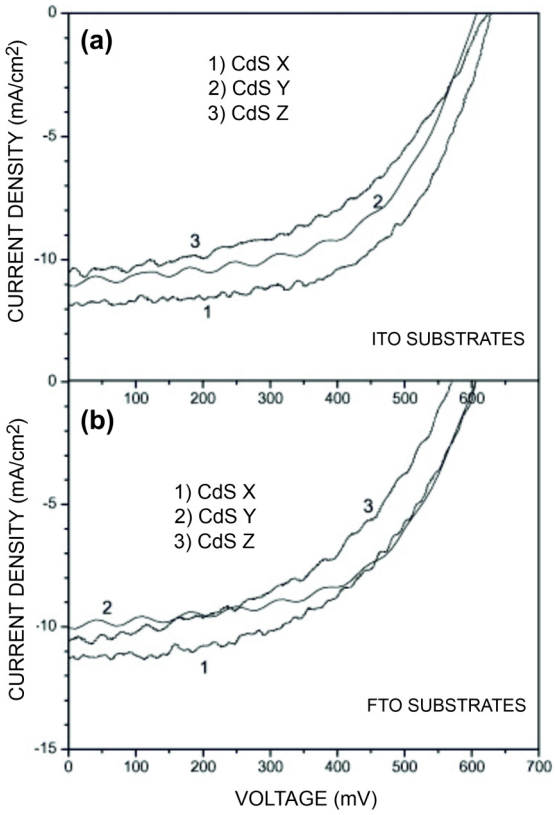

Fig. 13. J vs V measurements under AM 1.5 illumination of X, Y and Z solar cells deposited on (a) ITO and (b) FTO conductive glass substrates. Reproduced from Ref. 135.

Hernandez-Borja *et al.* [147] reported on the CdS/PbS film chemically deposited through an AF process. In PV cells, CdS and PbS were used as an active layer. They used sodium citrate to replace ammonia as the complexing agent. Potassium hydroxide was also used as ammonia substitute, but it did not affect essentially the efficiency of the PV cell. During the deposition, it did not help to reduce the use of poisonous and unsafe products, such as ammonia and triethanolamine. Authors fabricated a novel type of solar cell such as glass/ITO/CdS/PbS/conductive graphite. They deposited CdS as a window and PbS as absorption layers by the CBD technique. There were three different complexing agents used labeled as T, X, and Y. The T-CdS films were deposited as action solution comprising triethanolamine $C_6H_{15}NO_3$, and NH_4OH, for X-CdS films used sodium citrate $Na_3C_6H_5O_7$, instead of triethanolamine in a coating solution $Na_3C_6H_5O_7$, NH_4OH and the AF technique for the Y-CdS films deposition containing $Na_3C_6H_5O_7$, KOH, ammonium hydroxide NH_4OH.

Some researchers have generated a very convenient replacement of CBD processes for CdS and CdSe thin films growth [142-144,146,148]. In the recent CdTe/CdS solar cells' related papers, it is found that an AF chemically deposited CdS film as a window layer performed quite well [135,149,150]. PbS was found as an absorbent material that could be paired with CdS layer in different solar cells. In 1972, Watanabe and Mita [151] had already demonstrated the epitaxial development of PbS over CdS single crystals for applications in solar cell. The measured values of J_{sc} and V_{oc} under 3000 W/m^2 tungsten-halogen illumination were of 0.4 mA/cm^2 and 400 mV, respectively. Moreover, in 1980, Elabd and Steckl [152] also reported on the Si/PbS heterojunction with V_{oc} as of 8 mV and I_{sc} as of 0.2 mA. PbS is known as a thin band-gap semiconductor that shows excellent properties among the majority of semiconductors. PbS is another highly sensitive material with more grain size than standard semiconductors such as Si that makes it a better aspirant for producing nanostructured devices. Additionally, in nanostructures such as PbS, PbSe, etc., the impact of generation of multiple exciton was found [153] which is very promising for applications in solar cell.

Superstrate structure is used for fabricating the CdS/PbS solar cell showed in Fig. 14. PbS layer was deposited at the top of the cell with the back contact as four graphites and the ITO was used as the front contact. The area of the solar cells was of 0.16 cm^2. Usually, CdS films has n-type conductivity without special doping, while PbS has a p-type conductivity.

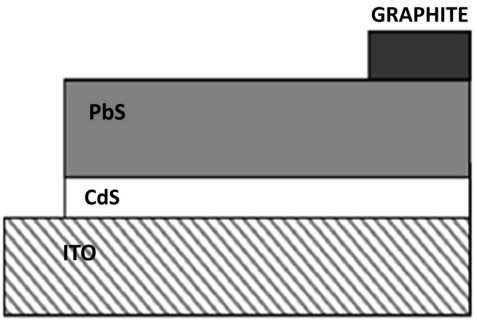

Fig. 14. Structure of the CdS/PbS solar cell. Reproduced from Ref. 147.

Figure 15 presents the J–V characteristics of different CdS films in the dark. A sharp rise in current is noticed at voltages about 0.3 V – 0.4 V, which is an indication that the barrier was of the 0.3 – 0.4 eV range. Below 90 mW/cm^2 tungsten-halogen illuminations, observed PV parameters for PbS/CdS solar cells are reported in Table 4. From Table it is clear that *FF* of the Y- type CdS cell is low, so there was an open field for cell optimization at the cost of its electrical parameters. The Y-type CdS cell was produced by the AF process. Because of the lesser *FF*, the performance of the Y- type CdS cell was precisely lower than that of the X-type CdS-based cell. However, the ratio of *FF* and the Z values were the same for both cells. It should be noted that small cell *FF* values could result from the same material porosity obtained by the CBD method, which enabled the impurities that affected electrical properties to be easily diffused.

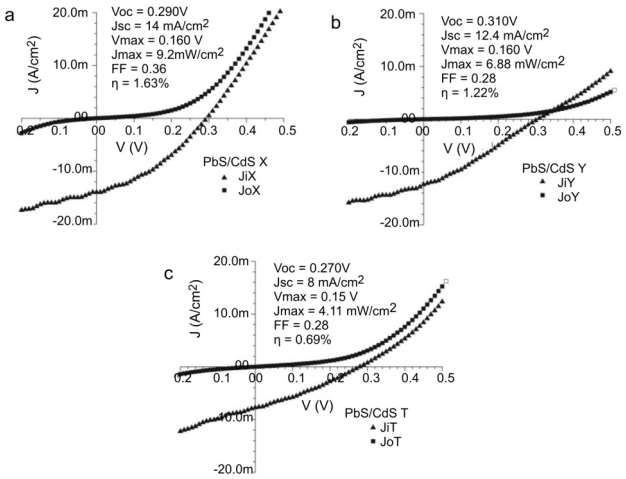

Fig. 15. J-V characteristics in the dark and under illumination of 90 mW/cm^2 of (a) CdS-X/PbS (b) CdS-Y/PbS, and (c) CdS-T/PbS solar cell. Reproduced from Ref. 147.

Table 4
PV parameters observed under 90 mW/cm^2 for PbS/CdS solar cells. Reproduced from Ref. 147.

Window layer	Parameters			
	V_{oc} (mV)	J_{sc} (mA/cm^2)	*FF*	*η(%)*
T-CdS	280	7.75	0.30	0.72
Y-CdS	310	12.37	0.28	1.22
X-CdS	290	14.00	0.36	1.63

As the literature suggests, Sandoval-Paz *et al.* [144] also explained about the AF process. The authors reported on the CdS films deposited by the AF CBD process. They tried to compare the optical and structural properties of CdS films at various deposition times obtained from two different CBD methods. In most recent papers the CdS films were deposited as a complexing agent by an AF CBD process using sodium citrate [142,143]. The authors found that an alkaline solution of $CdCl_2$, sodium citrate and thiourea can be used to obtain reliable and oriented CdS films. The CdS films obtained from the AF process displayed more similar properties and even improved compared with the CBD process based on ammonia. Authors analyzed a form of two varied layers:

(i) the AF reaction solution encouraged the method of ion deposition for high refractive index and very focused on CdS films. This was allocated to a pure compressed CdS layer and their optical properties were simulated by a Kramers–Kronig consistent model. Improvement of the AF CdS films begins with the formation after an induction period of a dense adhere layer using an ion by ion method. The observed layers' thickness was reported between 57 nm – 80 nm after the deposition of 15 – 120 min. The high refractive index validated the compactness of this layer, measured the AF CdS film which was deposited for 15 min.

(ii) the addition of ammonia and increasing amounts of Cd and S in the ammonia-containing (AC) reaction solution altered kinetic growth and resulted in faster colloid formation leading to cluster deposition. It was based on effective estimation of the Bruggeman medium. The flexible layer developed in the layer structure of AC CdS films since the very starting of the CBD process. This was the result of rapid colloid creation encouraged in the reaction solution by the changed chemical conditions. The lowest refractive index and the highest voids of the film were the outcomes of the process of cluster by cluster deposition for 15 min. Moreover, at this point, the film development was not defined as a favored crystalline orientation. In this case, the films were composed of a porous layer. It was observed that the crystalline orientation and refractive index were not as high as in the AF case. So, by this phenomenon, it is justified that AF CdS is much better than the AC CdS films as better and reliable window layers for the solar cells.

2.5. Enhancement of the window layer property

In conventional CdTe PV cells, CdS film is used as a heterojunction partner and a window layer material, because of its various advantages such as its high transparency, direct bandgap transition, high electron affinity, and n-type conductivity [154,155]. Since the energy range for solar irradiance is between 1.4 eV and 3 eV, the CdS bandgap (2.42 eV) is comparatively low, relative to this range. [156]. The photons can be absorbed with energy greater than 2.42 eV through the Cds layer, although the II-VI semiconductor compounds have absorption effectiveness up to 10^4 - 10^5 cm^{-1}. Photons with higher energies are absorbed on that plane where the recombination is considerable and depletion region is distant which makes a small contribution to the photocurrent [157].

As a window material, CdS is a highly recommended material because of its energy bandgap can be adjusted appropriately [158,159]. This acquires many fundamental qualities, such as moderate thickness, comparatively high transparency, increased photoconductivity and decreased loss of electric solar cells [160]. In CdS/CdTe thin film solar cell, CdS (as a window layer) plays a very essential role by following spectral response. It also works for the CdTe layer crystallinity and it felicitates the creation of broad energy bandgap ternary crystal layers near the interface of CdS–CdTe [161-163]. To enhance the performance of CdTe solar cells, there should be

established more appropriate window layer material. As it is known, energy bandgap value of CdS is of 2.4 eV and when the Zn (bandgap of 3.7 eV) incorporated into the CdS, it enhances the property of the material by making the ternary alloy [(Cd-Zn)S]. (Cd-Zn)S film with a larger bandgap absorbs a wider portion of the solar spectrum. Thus, it helps to circumvent the losses in window absorption and the lattice mismatch in a solar absorber layer [164,165]. The incorporation of Zn into CdS helps to improve the material's diffusion length and resistivity offering an optical window for an efficient heterojunction structure production [161].

Kartopu *et al*. [166] analyzed the effect of the ternary alloy (CdZnS) as a window layer in $Cd_{1-x}Zn_xS$/CdTe solar cells. With the aim to improve the efficiency of CdS/CdTe solar cells, even with the risk of increased pin-hole defects and shunting, CdS layer thinning was applied by the author. Their unconventional approach by forming the compositions of $Cd_{1-x}Zn_xS$ was to broaden the energy bandgap of the layer (window layer) so that it could permit higher energy photons to arrive at the next layer (absorber layer), thus improving the photocurrent. Authors observed a continual increase in the photocurrent generation in the blue to near ultra-violet (UV) region by the normalized external quantum efficiency spectra (EQE spectra).

Brooks *et al*. [167] also analyzed the role of the window layer in $Cd_{1-x}Zn_xS$/CdTe PV device. There are various literatures that have already reported on the (CdZnS) window layers in solar cell devices [164,168-171]. In comparison between $Cd_{1-x}Zn_xS$/CdTe against CdS/CdTe PV devices, due to the wider bandgap of ternary alloy, the increased blue response highlighted its advantage greater than the traditional CdS window layer in measurement spectra of EQE shown in Fig 16. A reverse reaction was observed in LBIC measurements when the authors compared 405 nm, over the similar region at 658 nm and 810 nm.

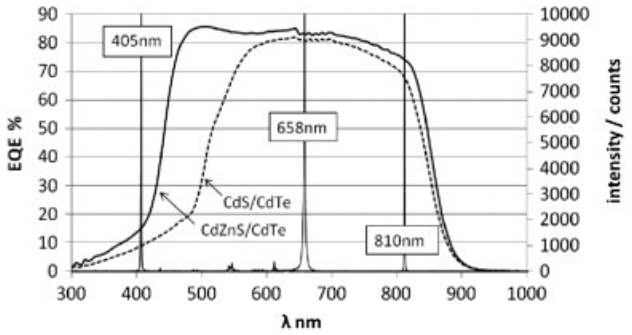

Fig. 16. EQE spectra of 240 nm $Cd_{1-x}Zn_xS$/2 mm CdTe and 240 nm CdS/2 mm CdTe devices and LBIC wavelengths used. Reproduced from Ref. 167.

The incident laser wavelengths were chosen for investigating varied SR of the full $Cd_{1-x}Zn_xS$/CdTe device. The IR laser was chosen to create photocurrent in the absorber layer and close to the bandgap of CdTe as shown in Figs. 16 and 17. Due to the absorption of the window layer and sensitivity to the window layer thickness, the EQE response was weak at approximately 45 nm under the $Cd_{1-x}Zn_xS$ band edge (λ = 405 nm). It is observed that both wavelengths (λ = 658 nm and 810 nm) were extremely translucent in the $Cd_{1-x}Zn_xS$ layer (window layer) and absorbent in the CdTe layer (absorber layer).

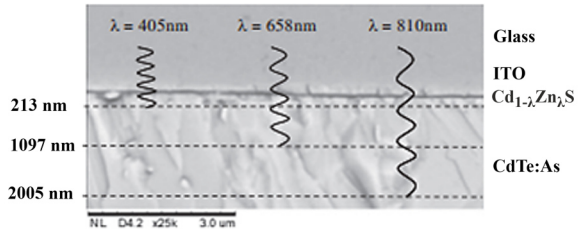

Fig. 17. Illustration of calculated photon penetration depth d_p into CdTe absorber layer for 3 wavelengths. Reproduced from Ref. 167.

Authors used a triple wavelength LBIC (laser beam induced current) mechanism to evaluate the $Cd_{1-x}Zn_xS$ distribution of thickness and to find out the impact of $Cd_{1-x}Zn_xS$ on efficiency and output current. They examined a sequence of devices where the thickness of $Cd_{1-x}Zn_xS$ ranged from 50 nm to 300 nm and showed a linear association between concentration of 300 nm $Cd_{1-x}Zn_xS$ and V_{oc} (Table 5). Followed by a maximum short wavelength reaction, a decrease at longer wavelengths was defined as a localized fall in V_{oc} due to a rise in the current of inverse saturation and a decreased lifetime of the minority carrier. It is shown that differences in overall cell conversion efficiencies depend on both V_{oc} and R_{sh}, although V_{oc} is effectively dependent on the thickness and distribution of $Cd_{1-x}Zn_xS$. V_{oc} exhibited a linear dependence on a 300 nm thick $Cd_{1-x}Zn_xS$ surface coverage. Here, R_{sh} trend was observed to be independent of these recognized defects and associated with a more complicated clustering of slighter defects.

Table 5
J–V results from devices (1–5). All results measured over full 5x5 cm^2 contact areas. Reproduced from Ref. 167.

Contact	η (%)	J_{sc} (mA/cm^2)	V_{oc} (mV)	FF (%)	R_s (Ω cm^2)	R_{sh} (Ω cm^2)
1	7.8	23.8	545	60.0	3.3	571
2	8.7	23.7	586	62.8	3.2	1685
3	9.3	23.6	667	59.3	3.8	1124
4	8.4	23.8	626	56.0	4.0	719
5	10.9	23.0	687	70.9	2.6	2005

In the less efficient devices, a non-uniform pinhole transmission accounts for low value of R_{sh} and would not link to the rate of large recombination in the absorber layer of CdTe of minority charge carriers, so as linked to thin $Cd_{1-x}Zn_xS$ window layer areas. The authors observed that highly efficient cells (> 10%) showed enhanced uniformity on photoresponse at all incident wavelengths. Here, a homogeneous $Cd_{1-x}Zn_xS$ film thickness was associated with greater efficient devices where localized 'spikes' remain at λ = 405 nm, showing places of pinholes with a

diameter of 100 mm in the window layer of $Cd_{1-x}Zn_xS$. In an association between V_{oc} and the thicker window layers coverage indicated that the using very thin window layers of $Cd_{1-x}Zn_xS$ in these devices would result in a punishment. Though, it is possible to use thicker window layers of $Cd_{1-x}Zn_xS$ without reducing J_{sc} with the shorter wavelength transmission of $Cd_{1-x}Zn_xS$.

Werta *et al*. [172] also explained the effect on the window layer by adding Zn into the CdS. They worked in three types of cathodic voltages (i) 1695 mV (ii) 1700 mV and (iii) 1705 mV. As the Zn was integrated into the CdS for making $Cd_{1-x}Zn_xS$ alloy, the energy bandgap progressively increased from 2.42 eV to 2.51 eV with the increasing voltage. This has demonstrated the suitability of the Cd1-xZnxS film as a window layer material in solar cells relative to the CdS film. Zn was considered to have a normal reduction potential of -760 mV and Cd has a reduction potential of -403 mV lower than Zn. In the reported paper, the $Cd_{1-x}Zn_xS$ film (where x = 0.98) was the Cd-rich at 1695 mV (low voltage deposition). On the other hand, more Zn was progressively integrated into the film with increasing voltages from 1700 mV and 1705 mV. Concurrently, the overall rate of deposition was decreased with a reduction in intensity of the diffraction peaks as shown in Fig. 18.

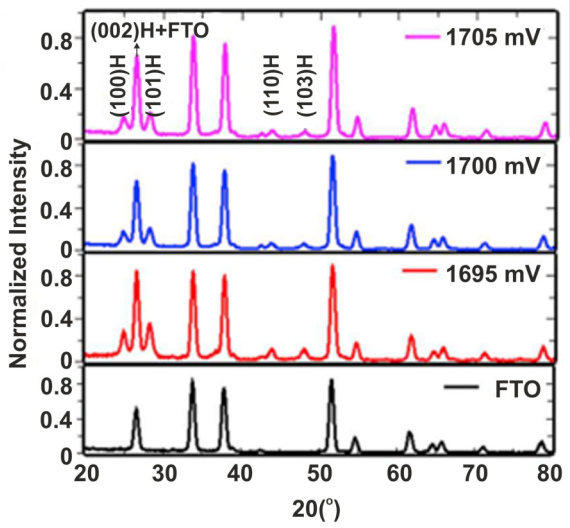

Fig. 18. GIXRD patterns of $Cd_{1-x}Zn_xS$ thin flms electrodeposited at a cathodic voltage of 1695 mV, 1700 mV and 1705 mV. Reproduced from Ref. 172.

The transmittance spectra of the $Cd_{1-x}Zn_xS$ thin films also explained the effect of Zn incorporation as shown in Fig. 19. With the increase in deposition voltage, Authors observed a considerable change in the transmittance, because of the integration of more Zn into the CdS film. Conversely, the absorbance spectral value decreased with an increase in deposition voltage. When the deposition voltage was increased, the thickness of the $Cd_{1-x}Zn_xS$ thin film decreased. Due to this fact, the film became less absorbing and highly transmitive. With the superiority of high transmitivity, $Cd_{1-x}Zn_xS$ became more suitable and beneficial for solar cells as a window layer material instead of CdS.

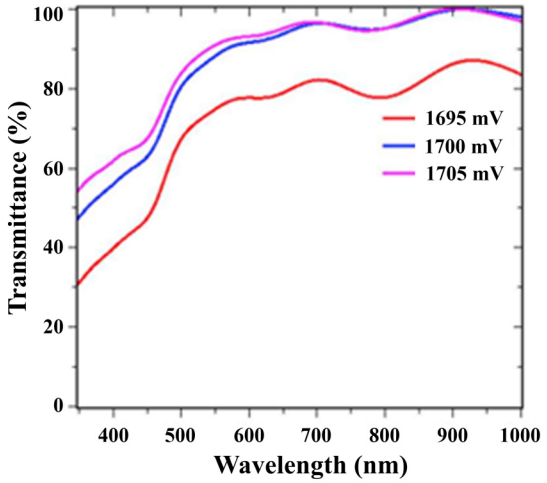

Fig. 19. Transmittance spectra of $Cd_{1-x}Zn_xS$ thin films as a function of deposition voltage. Reproduced from Ref. 172.

The authors observed two main features as the deposition voltage increased: (i) reduction in rate of deposition and (ii) integration of more Zn atoms. It is also reported that the energy bandgap increased with increasing deposition voltage resulting in the contribution of these two features. It is also well known that the bandgap of semiconductor materials is appreciably influenced by the films' thickness. Therefore, with an increase in deposition voltage, the increase in bandgap might be because of the reduction in the films' thickness. Authors demonstrated the association between the energy bandgap, voltage and incorporated Zn amount into the film as shown in Fig. 20. As explained earlier, the increase in deposition voltage incorporated Zn amount into the $Cd_{1-x}Zn_xS$ film increased and in the same way the energy bandgap of the films also increased. This showed the influence of the deposition voltage into the chemical and physical properties of the $Cd_{1-x}Zn_xS$ thin films prepared by electrodeposition technique. This implies the significance of the materials as the window layer for the solar cell.

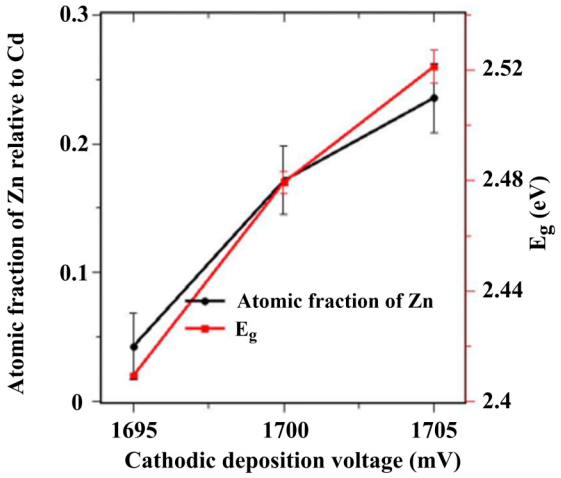

Fig. 20. Relative atomic fraction of Zn and energy bandgap (E_g) of $Cd_{1-x}Zn_xS$ thin films as a function of growth voltage. Reproduced from Ref. 172.

3. Future Scopes

From the above discussion, it is proved how important CdS is as a window layer and how much its corresponding aspects for improving the window layer are also very useful for PV cells. A thickness reduction of the active layer of CdS/CdTe thin film solar cells is one of the most essential requirements for reducing production costs and harmful influence of Cd toxicity. With the reduction in thickness, most of the photon energy will pass speedily and move to the absorber layer. Thus, much amount of photo-generation will occur. The presence of an HRT layer profoundly improves the quality of a thin CdS diode. A buffer or HRT layer decreases the thickness of the critical CdS and reduces the level of V_{oc} . Light-dark mixing occurs in the devices as the CdS thickness decreases and becomes more pronounced with lower V_{oc} . Under the solar illumination, CdTe solar cells are often degraded. Moreover, there is no proof of the mechanism of degradation due to its consistent appearance. To avoid this degradation of cells and get a reliable and reproducible efficiency, diffusion of Cu (from the back contact) into the CdS layer has to be under control. The following aspects are suggested to keep away the degradation: CdTe composition should be stochiometry and in case of any probability of vacancy, any defect in CdTe should be suppressed. For the device degradation: improvements to the CdTe/CdS interface often play a major role in addition to the back contact. Solar cells exposed to environmental conditions are also degraded, since the semiconductors and metal contacts used in the solar cell are oxidized and degraded. Inter-diffusion of the materials or accumulation of the ions at the junction (space charge region) or back contact also can cause degradation. Local environmental factors may also affect the worsening of PV parameters. Nano-wire acquires unique electronic and optical properties. Because of the large potential energy conversion efficiency and optical advantages, nano-wires are useful in the fabrication of PV devices. With the help of optical studies, it is evidenced that the CdS NWs arrays are shown to have appreciably greater transmittance for low-energy photons and their energy bandgap value changes to 3.5 eV. An improved transmission in PV devices through the window layer of the NWs array could results in a gain of about 20.6 % in the current provided by light. Additionally, it can be predicted that the CdS NW configuration would produce a gain of about 10.2 % in V_{oc} where interface recombination is the primary mechanism for electrons' transportation across the window/absorber junction. In the development of various PV systems, the production cost is also the most important factor. It includes material and technology costs, as well as energy consumption in various technological processes. Maintaining the ecological balance is important so that clean energy and clean technology are needed to support the devices. Thus, all the above requirements should be referred to the optimization of ammonia-free CBD processes. In these approaches ammonia or ammonia compounds can be substituted by other complexing agents, such as ethylenediamine, ethanolamine, triethanolamine, sodium citrate, and nitrilotriacetic acid. To improve the CdTe solar cells' performance, it is advised to use a wider bandgap material so that photons can easily transmit. There should be established a more appropriate window layer material. When Zn is incorporated into CdS, it enhances property of the material by making the ternary alloy [(Cd-Zn)S]. (Cd-Zn)S film with larger bandgap absorbs a wider portion of the solar spectrum so that it helps to avoid the window absorption losses and the lattice mismatch in a solar absorber layer. Incorporating Zn into CdS helps increase the material's resistivity and diffusion length, and also provides an optical window for manufacturing of heterojunction structure.

Acknowledgement

Authors are thankful to McCandles, K. Nakamura, J.M. Kephart, R. Mendoza-Perez, B.T. Ahn, H. Lin, H. Dang, P. Liu, R. Ochoa-Landin, J. Hernandez-Borja, G. Kartopu, W.S.M. Brooks, S.Z. Werta and their co-authors whose works have been reviewed here and to the publishers of the respective journals (Elsevier B. V. Netherland, IEEE, Wiley and Institute of Physics, America).

References

[1] Chornet, E. & Czernik, S. Harnessing hydrogen, *Nature* **418**, 928-929 (2002). https://doi.org/10.1038/418928a.

[2] Fujishima, A. & Honda, K. Electrochemical photolysis of water at a semiconductor electrode. *Nature* **238**, 37-38 (1972). https://doi.org/10.1038/238037a0.

[3] Bard, A. J. Photoelectrochemistry, *Science* **207**, 139-144 (1980), https://doi.org/10.1126/*science*.207.4427.139.

[4] Chen, X. B. Shen S. H., Guo L. J. & Mao S. S. Semiconductor-based Photocatalytic Hydrogen Generation. *Chem. Rev*. **110**, 6503-6570 (2010). https://doi.org/10.1021/cr1001645.

[5] Lewis, N.S. Toward cost-effective solar energy use. *Science* **315**, 798–801(2007), https://doi.org/10.1126/science.1137014.

[6] Lewis, N. S. & Nocera, D. G. Powering the planet: Chemical challenges in solar energy utilization. *Proc. Natl. Acad. Sci. USA* **103**, 15729–15735 (2006). https://doi.org/10.1073/pnas.0603395103.

[7] Deb, S. K. Dye-sensitized TiO2 thin-film solar *cell* research at the national renewable energy laboratory (NREL). *Sol. Energy Mater. Sol. Cells* **88**, 1–10 (2005). https://doi.org/10.1016/j.solmat.2004.09.007.

[8] Selinsky, R. S., Ding, Q., Faber, M. S., Wright, J. C. & Jin, S. Quantum dot nanoscale heterostructures for solar energy conversion, *Chem. Soc. Rev.* **42**, 2963–2985 (2013). https://doi.org/10.1039/C2CS35374A .

[9] Fang, Z., Wang, X. C., Wu H. C. & Zhao C. Z. Achievements and challenges of CdS/CdTe solar cells. *Int. J. Photoenergy* **2011**, 1-8 (2011). https://doi.org/10.1155/2011/297350 .

[10] Sharma, A. *PV demand database quarterly*. IMS Research 2011.

[11] Yan, B., Yue, G., Xu, X., Yang, J. & Guha, S. High efficiency amorphous and nanocrystalline silicon solar cells. *Physica Status Solidi A* **207**, 671–677 (2010). https://doi.org/10.1002/pssa.200982886.

[12] Green, M. A. Thin film solar cells: review of materials, technologies and commercial status. *J. Mater. Sci. Electron.* **18**, S15–S19 (2007). https://doi.org/10.1007/s10854-007-9177-9

[13] Fthenakis, V. Sustainability of photovoltaics: The case for thin-film solar cells. *Renew. Sustain. Energy Rev.* **13**, 2746–2750 (2009). https://doi.org/10.1016/j.rser.2009.05.001

[14] Kietzke, T. Recent Advances in Organic Solar Cells. *Adv. in optoElectron.* **2007**, 40285 (2007). https://doi.org/10.1155/2007/40285.

[15] Ren, L. & Wang, S. Progress of organic photovoltaic materials. *Recent Patents on Mater. Sci.* **3**, 26–39 (2010). https://doi.org/10.2174/1874464811003010026.

[16] Kimbis, T. P. *Solar energy technology program*. US Department of Energy (2011).

[17] Aurvtin, V., Izyumskaya, N. & Moroko, H. Semiconductor solar cells: Recent progress in terrestrial applications. *Superlatt. Microstruct.* **49**, 337-364 (2011). https://doi.org/10.1016/j.spmi.2010.12.011.

[18] Fahrenbruch, A. L. & Bube, R. H. *Fundamentals of Solar Cells*. Academic Press, New York, USA (1983).

[19] Jeffery, L. G., Richard, J. S. & Youn, J. L. *Numerical modeling of $CuInSe_2$ and CdTe solar cells*. ECE Technical Reports (1994).

[20] Zia, R., Farhat, S., Shahzad, N. & Madeeha R. Improve the efficiency of CdTe/$Zn_xCd_{1-x}S$ all thin films solar cell by annealing. *Optik* **127**, 4502–4505 (2016). https://doi.org/10.1016/j.ijleo.2016.01.154

[21] Akbarnejad, E., Ghorannevis, Z., Mohammadi, E. & Fekriaval, L. Correlation between different CdTe nanostructures and the performances of solar cells based on CdTe/CdS heterojunction. *J. Electroanalytical Chem.* **849,** 113358 (2019). https://doi.org/10.1016/j.jelechem.2019.113358.

[22] Khare, A. & Bhushan, S. Effect of KI/LiF/$CdCl_2$ on photoluminescent and electroluminescent properties of nanocrystalline (Zn-Cd)S: Cu films. *Radiat Eff. Defects Solids* **161**, 631–644 (2006). https://doi.org/10.1080/10420150600874923.

[23] Li, H. & Xiangxin, L. Improved performance of CdTe solar cells with CdS treatment. *Sol. Energy* **115**, 603–612 (2015). https://doi.org/10.1016/j.solener.2015.02.044.

[24] Zhang, R., Wang, B., Wei, L., Li, X., Xu, Q., Peng, S., Kurash, I. & Qian, H. Growth and properties of ZnS thin films by sulfidation of sputter deposited Zn. *Vacuum* **86**, 1210–1214 (2012). https://doi.org/10.1016/j.vacuum.2011.11.003.

[25] Azizi, S., Rezagholipour Dizaji H. & Ehsani M. H. Structural and optical properties of $Cd_{1-x}Zn_xS$ (x = 0, 0.4, 0.8 and 1) thin films prepared using the precursor obtained from microwave irradiation processes. *Optik* **127**, 7104–7114 (2016). https://doi.org/10.1016/j.ijleo.2016.05.030.

[26] Lilhare, D., Sinha, T., & Khare, A. Influence of Cu doping on optical properties of (Cd–Zn)S nanocrystalline thin films: a review. *J. Mater. Sci: Mater. Electron* **29**, 688–713 (2018). https://doi.org/10.1007/s10854-017-7963-6.

[27] Perna, G., Capozzi, V., Ambrico, M., Augelli, V., Ligonzo, T., Minafra, A., Schiavulli, L. & Pallara, M. Structural and optical characterization of undoped and indium-doped CdS films grown by pulsed laser deposition. *Thin Solid Films* **453-454**, 187-194 (2004). https://doi.org/10.1016/j.tsf.2003.11.105.

[28] Opanasyuk, A. S., Kurbatov, D. I., Ivashchenko, M. M. & Protsenko, I. Y. Properties of the window layers for the CZTSe and CZTS based solar cells. *J. Nano Electron. Phys.* **4** 01024-01026 (2012).

[29] Sasikala, G., Thilakan, P. & Subramanian, C. Modification in the chemical bath deposition apparatus, growth and characterization of CdS semiconducting thin films for photovoltaic applications. *Sol. Energy Mater. Sol. Cells* **62**, 275-293 (2000) https://doi.org/10.1016/S0927-0248(99)00170-1

[30] Sinha, T., Lilhare, D. & Khare, A. A review on the improvement in performance of CdTe/CdS thin-film solar cells through optimization of structural parameters. *J. Mater. Sci.* **54**, 12189–12205 (2019). https://doi.org/10.1007/s10853-019-03651-0

[31] Khosroabadi, S. & Keshmiri, S. H. Design of a high efficiency ultrathin cds/cdte solar cell using back surface field and backside distributed bragg reflector. *Opt. express* **22**, A921-A929 (2014). https://doi.org/10.1364/OE.22.00A921

[32] McCandless, B. E. & Dobson, K. D. Processing options for CdTe thin film solar cells. *Sol. Energy* **77**, 839-856 (2004). https://doi.org/10.1016/j.solener.2004.04.012.

[33] Ferekides, S. C., Balasubramanian, U., Mamazza, R., Viswanathan, V., Zhao, H. & Morel, L. D. CdTe thin film solar cells: device and technology issues. *Sol. Energy* **77**, 823–830 (2004). https://doi.org/10.1016/j.solener.2004.05.023.

[34] Moller, H. J. *Semiconductor for Solar Cells*. Artech House, Boston (1993).

[35] Ray, B. *II-VI Compounds*. Pergamon Press, Oxford (1969).

[36] Albright, S., Ackerman, B. & Jordan, J. IEEE *Trans. Electron Devices* **ED-37**, 434 (1990).

[37] Morris, G., Tanner, P. & Tottszer, A. Proc. 21st IEEE PVSC, 575 (1990).

[38] Turner, A., Woodcock, J., Ozsan, M., Summers, J., Barker, J., Binns, S., Buchanan, K., Chai, C., Dennison, S., Hart, R., Johnson, D., Marshall, R., Oktik, S., Patterson, M., Perks, R., Roberts, S., Sadeghi, M., Sherborne, J., Szubert, J. & Webster, S. *Technical Digest of the International PVSEC-5*. (Kyoto, Japan) 761 (1990).

[39] McCandless, B. E. & Hegedus, S. S. 22nd IEEE PV. Specialists Conference. Institute of Electrical and ElectronicsEngineers, New York, 967–972 (1991).

[40] McCandless, B. & Birkmire R. Analysis of post deposition processing for CdTe/CdS thin film solar cells. *Sol. Cells* **31**, 527-535 (1991). https://doi.org/10.1016/0379-6787(91)90095-7

[41] Nakamura, K., Gotoh, M., Fujihara, T., Toyama, T. & Okamoto, H. Influence of CdS window layer on 2-μm thick CdS/CdTe thin film solar cells. *Sol. Energy Mater. Sol. Cells* **75** 185–192 (2003). https://doi.org/10.1016/S0927-0248(02)00154-X

[42] Kephart, J. M., Geisthardt, R. M., Ma, Z., McCamy, J. & Sampath, W. S. Reduction of window layer optical losses in CdS/CdTe solar cells using a float-line manufacturable HRT layer. *IEEE*, 1653-1657 (2013). https://doi.org/10.1109/PVSC.2013.6744462.

[43] Wu, X., Asher, S., Levi, D. H., King, D. E., Yan, Y., Gessert, T. A. & Sheldon, P. Interdiffusion of CdS and Zn_2SnO_4 layers and its application in CdS/CdTe polycrystalline thin-film solar cells. *J. Appl. Phys.* **89**, 4564–4569 (2001). https://doi.org/10.1063/1.1351539.

[44] Kartopu, G., Williams, B. L., Zardetto, V., Gurlek, A. K., Clayton, A. J., Jones, S., Kessels, W. M. M., Creatore, M. & Irvine, S. J. C. Enhancement of the photocurrent and efficiency of CdTe solar cells suppressing the front contact reflection using a highly-resistive ZnO buffer layer. *Sol. Energy Mater. Sol. Cells*, **191**, 78–82 (2019). https://doi.org/10.1016/j.solmat.2018.11.002.

[45] Dharmadasa, I. M., Madugu, M. L., Olusola, O. I., Echendu, O. K., Dahiru, F. F., Diso, G., Weerasinghe, A. R., Druffel, T., Dharmadasa, R., Lavery, B., Jasinski, J. B., Krentsel, T. A. & Sumanasekera, G. Electroplating of CdTe thin films from cadmium sulphate precursor and comparison of layers grown by 3-electrode and 2-electrode systems. *Coatings* **7**, 1-17 (2017). https://doi.org/10.3390/coatings7020017.

[46] Yang, R., Wang, D., Wan, L. & Wang, D. High-efficiency CdTe thin-film solar cell with a mono-grained CdS window layer. *RSC Adv.* **4**, 22162-22171 (2014). https://doi.org/10.1039/C4RA01394H.

[47] Limmanee, A., Songtrai, S., Udomdachanut, N., Kaewniyompanit, S., Sato, Y., Nakaishi, M., Kittisontirak, S., Sriprapha, K. & Sakamoto, Y. Degradation analysis of photovoltaic modules under tropical climatic conditions and its impacts on LCOE. *Renew. Energy* **102**, 199-204 (2017). https://doi.org/10.1016/j.renene.2016.10.052

[48] Sharma, V. & Chandel, S. S. A novel study for determining early life degradation of multi-crystalline-silicon photovoltaic modules observed in western himalayan indian climatic conditions. *Sol. Energy* **134,** 32-44 (2016). https://doi.org/10.1016/j.solener.2016.04.023.

[49] Balaska, A., Tahri, A., Tahri, F. & Stambouli, A. B. Performance assessment of five different photovoltaic module technologies under outdoor conditions in algeria. *Renew. Energy* **107**, 53-60 (2017). https://doi.org/10.1016/j.renene.2017.01.057.

[50] Silvestre, S., Kichou, S., Guglielminotti, L., Nofuentes, G. & Alonso-Abella, M. Degradation analysis of thin film photovoltaic modules under outdoor long term exposure in spanish continental climate conditions. *Solar Energy* **139** 599-607 (2016). https://doi.org/10.1016/j.solener.2016.10.030.

[51] Limmanee, A., Udomdachanut, N., Songtrai, S., Kaewniyompanit, S., Sato, Y., Nakaishi, M., Kittisontirak, S., Sriprapha, K. & Sakamoto, Y. Field performance and degradation rates of different types of photovoltaic modules: a case study in Thailand. *Renew. Energy* **89**, 12-17 (2016). https://doi.org/10.1016/j.renene.2015.11.088.

[52] Mendoza-Perez, R., Sastre-Hernandez, J., Contreras-Puente, G. & Vigil, G. O. CdTe solar cell degradation studies with the use of CdS as the window material. *Sol. Energy Mater. Sol. Cells* **93**, 79–84 (2009). https://doi.org/10.1016/j.solmat.2008.09.016.

[53] Romeo, N., Bosio, A., Tedeschi, R. & Canevari, V. Back contacts to CSS CdS/CdTe solar cells and stability of performances. *Thin Solid Films* **361–362**, 327–329 (2000). https://doi.org/10.1016/S0040-6090(99)00765-8.

[54] Singh, V. P., Erickson, O. M. & Chao, J. H. Analysis of contact degradation at the CdTe-electrode interface in thin-film CdTe-CdS solar-cells. *J. Appl. Phys.* **78**, 4538–4542 (1995). https://doi.org/10.1063/1.359796.

[55] Ahn, B. T., Yun, J. H., Cha, E. S. & Park, K. C. Understanding the junction degradation mechanism in CdS/CdTe solar cells using a Cd-deficient CdTe layer. *Curr. Appl. Phys.* **12**, 174-178 (2012). https://doi.org/10.1016/j.cap.2011.05.031.

[56] Visoly-Fisher, I., Dobson, K. D., Nair, J., Bezalel, E., Hodes, G. & Cahen, D. Factors affecting the stability of CdTe/CdS solar cells deduced from stress tests at elevated temperature. *Adv. Funct. Mater.* **13**, 289-299 (2003). https://doi.org/10.1002/adfm.200304259.

[57] Lyubomirsky, I., Ranbinal, M. K. & Cahen, D. Room-temperature detection of mobile impurities in compound semiconductors by transient ion drift. *J. Appl. Phys.* **81**, 6684-6691 (1997). https://doi.org/10.1063/1.365563.

[58] Romero, M. J., Albin, D. S., Al-Jassim, M. M., Wu, X., Moutinho, H. R. & Dhere, R. G. Cathodoluminescence of Cu diffusion in CdTe thin films for CdTe/CdS solar cells. *Appl. Phys. Lett.* **81**, 2962-2964 (2002). https://doi.org/10.1063/1.1515119.

[59] Wu, X., Keane, J. C., Dhere, R. G., DeHart, C., Albin, D. S., Duda, A., Gessert, T. A., Asher, S., Levi, D. H. & Sheldon, P. 16.5% Efficient CdS/CdTe polycrystalline thin film solar cell. in: *Proceedings of the 17th IEEE European PV Solar Energy Conference*, Munich, Germany, 995–1000 (2001).

[60] Lin, H., Irfan, Xia, W., Wu, H. N., Gao, Y. & Tang, C. W. MoO_x back contact for CdS/CdTe thin film solar cells: Preparation, device characteristics, and stability. *Sol. Energy Mater. Sol. Cells* **99**, 349–355 (2012). https://doi.org/10.1016/j.solmat.2012.01.001.

[61] Kroger, M., Hamwi, S., Meyer, J., Riedl, T., Kowalsky, W., & Kahn, A. Role of the deep-lying electronic states of MoO3 in the enhancement of hole-injection in organic thin films. *Appl. Phys. Lett.* **95,** 123301/1–123301/3 (2009). https://doi.org/10.1063/1.3231928.

[62] Zhang, M. L., Irfan, Ding, H. J., Gao, Y. L. & Tang, C. W. Organic Schottky barrier photovoltaic cells based on MoOx/C60. *Appl. Phys. Lett.* **96**, 183301/1–183301/3 (2010). https://doi.org/10.1063/1.3415497.

[63] Wang, Q. Hot-wire CVD amorphous Si materials for solar cell application. *Thin Solid Films* **517**, 3570–3574 (2009). https://doi.org/10.1016/j.tsf.2009.01.072.

[64] Bai, Y., Cao, Y., Zhang, J., Wang, M., Li, R., Wang, P., Zakeeruddin, S. M. & Gratzel, M. High-performance dye-sensitized solar cells based on solvent-free electrolytes produced from eutectic melts. *Nat. Mater.* **7**, 626–630 (2008). https://doi.org/10.1038/nmat2224.

[65] Wang, Q. High-efficiency hydrogeneated amorphous/crystalline Si heterojunction solar cells. *Phil. Mag.* **89**, 2587–2598 (2009). https://doi.org/10.1080/14786430902919489.

[66] Gessert, T. A., Metzger, W. K., Dippo, P., Asher, S. E., Dhere, R. G. & Young, M. R. Dependence of carrier lifetime on Cu-contacting temperature and ZnTe:Cu thickness in CdS/CdTe thin film solar cells. *Thin Solid Films* **517**, 2370–2373 (2009). https://doi.org/10.1016/j.tsf.2008.11.008.

[67] Singh, V. P., Linam, D. L., Dils, D. W., McClure, J. C. & Lush, G. B. Electro-optical characterization and modeling of thin film CdS–CdTe heterojunction solar cells. *Sol. Energy Mater. Sol. Cells* **63**, 445–466 (2000). https://doi.org/10.1016/S0927-0248(00)00063-5.

[68] Aliyu, M. M., Islam, M. A., Hamzah, N. R., Karim, M. R., Matin, M. A., Sopian, K. & Amin, N. Recent developments of flexible CdTe solar cells on metallic substrates: Issues and Prospects. *Int. J. photoenergy* **2012**, 1-10, (2012). https://doi.org/10.1155/2012/351381.

[69] Singh, V. P. & McClure, J. *Design issues* in the *fabrication* of *CdS–CdTe solar cells* on molybdenum foil substrates. *Sol. Energy Mater. Sol. Cells* **76**, 369–385 (2003). https://doi.org/10.1016%2FS0927-0248(02)00289-1.

[70] Metzger, W. K., Repins, I. L., Romero, M. & Dippo, P. Contreras, M., Noufi, R., Levi, D., Recombination kinetics and stability in polycrystalline Cu(In,Ga)Se2 solar cells, *Thin Solid Films* **517**, 2360–2364 (2009). https://doi.org/10.1016/j.tsf.2008.11.050.

[71] Green, M. A., Emery, K., Hishikawa, Y. & Warta, W. Solar cell efficiency tables (version 35). *Prog. Photovolt. Res. Appl.* 18, 144–150 (2010). https://doi.org/10.1002/pip.974.

[72] Garnett, E. & Yang, P., Light Trapping in Silicon Nanowire Solar Cells, *Nano Lett.* **10**, 1082–1087(2010). https://doi.org/10.1021/nl100161z.

[73] Liu, P., Singh, V. P., Rajaputra, S., Phok, S. & Chen Z. Characteristics of copper indium diselenide nanowires embedded in porous alumina templates. *J. Mater. Res.* **25**, 207–212 (2010). https://doi.org/10.1557/JMR.2010.0030.

[74] Law, M., Greene, L. E., Johnson, J. C., Saykally, R. & Yang, P. D. Nanowire dye-sensitized solar cells. *Nat. Mater.* **4**, 455–459 (2005). https://doi.org/10.1038/nmat1387.

[75] Tian, B. Z., Zheng, X., Kempa, T. J., Fang, Y., Yu, N., Yu, G., Huang, J. & Lieber, C. M. Coaxial silicon nanowires as solar cells and nanoelectronic power sources. *Nature* **449**, 885–889 (2007). https://doi.org/10.1038/nature06181.

[76] Xia, Y., Yang, P., Sun, Y., Wu, Y., Mayers, B., Gates, B., Yin, Y., Kim, F. & Yan, H. One-dimensional nanostructures: synthesis, characterization, and applications. *Adv. mater.*, **15**, 353-389 (2003). https://doi.org/10.1002/adma.200390087.

[77] Khare, A., Sahub, R. B. & Sharma, S. K. Effect of NaF on optical and structural properties of $Cd_xZn_{1-x}S$ nano crystalline films. *Optik* **123**, 1133– 1137 (2012). https://doi.org/10.1016/j.ijleo.2011.07.039.

[78] Morales, A. M. & Liber, C. M. A laser ablation method for the synthesis of crystalline semiconductor nanowires. *Science* **279**, 208-211 (1998). https://doi.org/10.1126/science.279.5348.208.

[79] Pan, Z. W., Dai, Z. R. & Wang, Z. L. Nanobelts of semiconducting oxides. *Science* **291**, 1947–1949 (2001). https://doi.org/10.1126/science.1058120.

[80] Huynh, W. U., Dittmer, J. J. & Alivisatos, A. P. Hybrid nanorod-polymer solar cells. *Science* **295**, 2425–2427 (2002). https://doi.org/10.1126/science.1069156.

[81] Nag, B. R. *Physics of Quantum Well devices*. Kluwer, Dordrecht, The Nederlands (2000).

[82] Herman, M. A. & Sitter, H. *Molecular Beam Epitaxy: Fundamental and current status*,. Springer, Berlin (1996).

[83] Alivisatos, P. Colloidal quantum dots. From scaling laws to biological applications. *Pure Appl. Chem.* **72**, 3-9 (2000). https://doi.org/10.1351/pac200072010003.

[84] Notzel, R. & Ploog K. Direct synthesis of semiconductor quantum-wire and quantum-dot structures. *Adv. Mater.* **5**, 22-29 (1993). https://doi.org/10.1002/adma.19930050104.

[85] Xu, D., Chen, D., Xu, Y., Shi, X., Guo, G., Gui, L. & Tang, Y. Preparation of II-VI group semiconductor nanowire arrays by dc electrochemical deposition in porous aluminum oxide templates, *Pure Appl. Chem.* **72**, 127-135 (2000). https://doi.org/10.1351/pac200072010127.

[86] Hiruma, K., Yazawa, M., Katsuyama, T., K., Okawa, Haraguchi, K., Kogucchi, M. & Kakibayashi, H. Growth and optical properties of nanometer-scale GaAs and InAs whiskers. *J. Appl. Phys.* **77**, 477-482 (1995). https://doi.org/10.1063/1.359026.

[87] Chen, J. *Investigation of CdS nanowires and planar films for enhanced performance as window layers in CdS-CdTe solar cell devices*. UKnowledge, June (2013) (Master's Thesis).

[88] Acharya, S., Patla, I., Kost, J., Efrima, S. & Golan, Y. Switchable assembly of ultra-narrow CdS nanowires and nanorods. *J. Am. Chem. Soc.* **128**, 9294-9295 (2006). https://doi.org/10.1021/ja062404i.

[89] Kar, S., Pal, B. N., Chaudhuri, S. & Chakravorty D. One-dimensional ZnO nanostructure arrays: synthesis and characterization. J.*Phys. Chem. B* **110**, 4605-4611 (2006). https://doi.org/10.1021/jp056673r.

[90] Rao, C. N. R., Deepak, F. L., Gundiah, G. & Govindaraj, A. Inorganic nanowires. *Prog. Sol. State Chem.* **31**, 5-147 (2003). https://doi.org/10.1016/j.progsolidstchem.2003.08.001.

[91] Zeiri, L., Patla, I., Acharya, S., Golan, Y. & Efrima, S. Raman spectroscopy of ultranarrow CdS nanostructures. *J. Phys. Chem. C* **111**, 11843-11848 (2007). https://doi.org/10.1021/jp072015q.

[92] Wong, E. W., Sheehan, P. E. & Lieber, C. M. Nanobeam mechanics: elasticity, strength, and toughness of nanorods and nanotubes. *Science* **277**, 1971-1975 (1997). https://doi.org/10.1126/science.277.5334.1971

[93] Colvin, V. L., Schlamp, M. C. & Alivisatos, A. P. Light-emitting diodes made from cadmium selenide nanocrystals and a

semiconducting polymer. *Nature* **370**, 354-357 (1994). https://doi.org/10.1038/370354a0.

[94] Klein, D. L., Roth, R., Lim, A. K. L., Alivisatos, A. P. & McEuen, P. L. A single-electron transistor made from a cadmium selenide nanocrystals. *Nature* **389**, 699-701 (1997). https://doi.org/10.1038/39535.

[95] Ridley, B. A., Nivi, B. & Jacobson, J. M. All-inorganic field effect transistors fabricated by printing. *Science* **286**, 746-749 (1999). https://doi.org/10.1126/science.286.5440.746.

[96] Alivisatos, A. P. Semiconductor Clusters, Nanocrystals, and Quantum Dots. *Science* **271**, 933-937 (1996). https://doi.org/10.1126/science.271.5251.933.

[97] Xu, D., Xu, Y., Chen, D., Guo, G., Gui, L. & Tang, Y. Preparation and characterization of CdS nanowire arrays by dc electrodeposit in porous anodic aluminium oxide templates. *Chem. Phys. Lett.* **325**, 340-344 (2000). https://doi.org/10.1016/S0009-2614(00)00676-X.

[98] Guduru, S., Singh, V., Rajaputra, S., Mishra, S. & Mangu, R. Characteristics of gold/cadmium sulfide nanowire Schottky diodes. *Thin Solid Films* 518, 1809-1814 (2010). https://doi.org/10.1016/j.tsf.2009.09.038.

[99] Tian, B. Z., Zheng, X. L., Kempa, T. J., Fang, Y., Yu, N. F., Yu, G. H., Huang, J. L. & Lieber, C. M. Coaxial silicon nanowires as solar cells and nanoelectronic power sources. *Nature* **449**, 885–890 (2007). https://doi.org/10.1038/nature06181.

[100] Kelzenberg, M. D., Boettcher, S. W., Petykiewicz, J. A., Turner-Evans, D. B., Putnam, M. C., Warren, E. L., Spurgeon, J. M., Briggs, R. M., Lewis, N. S. & Atwater, H. A. Enhanced absorption and carrier collection in Si wire arrays for photovoltaic applications. *Nat. Mater.* **9**, 239–244 (2010). https://doi.org/10.1038/nmat2635

[101] Fan, Z., Razavi H., Do, J. W., Moriwaki, A., Ergen, O., Chueh, Y. L., Leu, P. W., Ho, J. C., Takahashi, T., Reichertz, L. A., Neale, S., Yu, K., Wu, M., Ager, J. W. & Javey, A. Three-dimensional nanopillar-array photovoltaics on low-cost and flexible substrates. *Nat. Mater.* **8**, 648–653 (2009). https://doi.org/10.1038/nmat2493.

[102] Zhu, J., Hsu, C. M., Yu, Z. F. & Fan, S. H. Cui, Y. Nanodome Solar Cells with Efficient Light Management and Self-Cleaning. *Nano Lett.* **10**, 1979–1984 (2010). https://doi.org/10.1021/nl9034237.

[103] Ni, L., Jacques, E., Rogela, R., Salaun, A. C., Pichon, L. & Wenga, G. VLS silicon nanowires based resistors for chemical sensor applications. *Procedia Engineering* **47**, 240–243 (2012). https://doi.org/10.1016/j.proeng.2012.09.128.

[104] Dang, H., Singh, V., Rajaputra, S., Guduru, S., Chen, J. & Nadimpally, B. Cadmium sulfide nanowire arrays for window layer applications in solar cells, *Sol. Energy Mater. Sol. Cells* **126**, 184–191 (2014). https://doi.org/https://doi.org/10.1016/j.solmat.2014.03.039

[105] Liu, P., Singh, V. P., Jarro, A. C. & Rajaputra, S. Cadmium sulfide nanowires for the window semiconductor layer in thin film CdS-CdTe solar cells. *Nanotechnology* **22**, 145304 (2011). https://doi.org/10.1088/0957-4484/22/14/145304.

[106] Fan, Z., Ruebusch, D. J., Rathore, A. A., Kapadia, R., Ergen, O., Leu, P. W. & Javey, A. Challenges and prospects of nanopillar-based solar cells. *Nano Res.* **2**, 829–843 (2009). https://doi.org/10.1007/s12274-009-9091-y.

[107] Wu, X., Zhou, J., Duda, A., Keane, J. C., Gessert, T. A., Yan, Y. & Noufi, R. 13·9%-efficient CdTe polycrystalline thin-film solar cells with an infrared transmission of ~50%, *Prog. Photovolt., Res. Appl.* **14**, 471–483 (2006). https://doi.org/10.1002/pip.664.

[108] Zhu, Y., Li, Z., Chen, M., Cooper, H. M., Lu, G. Q. & Xu, Z. P. One-pot preparation of highly fluorescent cadmium telluride/cadmium sulfide quantum dots under neutral-pH condition for biological applications. *J. Colloid Interf. Sci.* **390**, 3-10 (2013). https://doi.org/10.1016/j.jcis.2012.08.003.

[109] Garnett, E. & Yang, P. D. Light trapping in silicon nanowire solar cells. *Nano Lett.* **10**, 1082–1087 (2010). https://doi.org/10.1021/nl100161z.

[110] Hu, L. & Chen, G. Analysis of optical absorption in silicon nanowire arrays for photovoltaic applications. *Nano Lett.* **7**, 3249-3252 (2007). https://doi.org/10.1021/nl071018b

[111] Sahoo, M. K. & Kale, P. Integration of silicon nanowires in solar cell structure for efficiency enhancement: A review**.** *J. Materiomics* **5**, 34-48 (2019). https://doi.org/10.1016/j.jmat.2018.11.007.

[112] Tang, J., Huo, Z., Brittman, S., Gao, H. & Yang P. Solution-processed core-shell nanowires for efficient photovoltaic cells. *Nat. Nanotechnol.* **6**, 568–572 (2011). https://doi.org/10.1038/nnano.2011.139.

[113] Lilhare, D., Sinha T.,Verma, L. & Khare, A. Optimization of Zn concentration in chemically deposited $(Cd_x–Zn_{1–x})S$ nanocrystalline films for solar cell applications. *Semicond. Sci. Tech.* **34**, 125010 **(**2019). https://doi.org/10.1088/1361-6641/ab4aea

[114] Sze, S. M. & Kwok, K. N. *Physics of Semiconductor Devices*. 3rd edn, New York: Wiley, (2007).

[115] Romeo, A., Batzner, D. L., Zogg, H., Vignali, C. &Tiwari A. N. Influence of CdS growth process on structural and photovoltaic properties of CdTe/CdS solar cells. *Sol. Energy Mater. Sol. Cells* **67**, 311-321 (2001). https://doi.org/10.1016/S0927-0248(00)00297-X.

[116] Contreras, M. A., Romero, M. J., To, B., Hasoon, F., Hasoon, R. Noufi, Ward, S. & Ramanathan, K. Optimization of CBD CdS process in high-efficiency $Cu(In,Ga)Se_2$ based solar cells. *Thin Solid Films* **403-404**, 204-211 (2002). https://doi.org/10.1016/S0040-6090(01)01538-3

[117] Perez, R. M., Hernandez, J. A., Hernandez, J. S., Quiebras, N. X., Puente, G. C., Rodrıguez, G. S., Galan, O. V., Garcıa, E. M. & Acevedo, A. M. Photoluminescence characteristics of CdS layers deposited in a chemical bath and their correlation to CdS/CdTe solar cell performance. *Sol. Energy* **80**, 682-686 (2006). https://doi.org/10.1016/j.solener.2006.01.002.

[118] Bayhan, H. & Kavasoglu, A. S. Study of CdS/Cu(In, Ga)Se 2 heterojunction interface using admittance and impedance spectroscopy. *Sol. Energy* **80**, 1160-1164 (2006). https://doi.org/10.1016/j.solener.2005.09.004

[119] Borja, J. H., Vorobiev, Y. V. & Bon, R. R. Thin film solar cells of CdS/PbS chemically deposited by an ammonia-free process. *Sol. Energy Mater. Sol. Cells* **95**, 1882–1888 (2011). https://doi.org/10.1016/j.solmat.2011.02.012.

[120] Hiie, J., Dedova, T., Valdna, V. & Muska, K. Comparative study of nano-structured CdS thin films prepared by CBD and spray pyrolysis: Annealing effect. *Thin Solid Films* **511**, 443–447 (2006). https://doi.org/10.1016/j.tsf.2005.11.070.

[121] Kalandaragh, Y. A., Muradov, M. B., Mammedov, R. K. & Khodayari, A. Growth process and investigation of some physical properties of CdS nanocrystals formed in polymer matrix by successive ionic layer adsorption and reaction (SILAR) method. *J. Cryst. Growth* **305**, 175–180 (2007). https://doi.org/10.1016/j.jcrysgro.2007.03.010

[122] Kaur, I., Pandya, D. K. & Chopra, K. L. Growth kinetics and polymorphism of chemically deposited CdS films. *J. Electrochem. Soc.* **127**, 943–948 (1980). https://doi.org/10.1149/1.2129792.

[123] Borges, R. O. & Lincot D. Mechanism of chemical bath deposition of cadmium sulfide thin films in the ammonia-thiourea system. *J. Electrochem. Soc.* **140**, 3464–3473 (1993). https://doi.org/10.1149/1.2221111.

[124] Brien, P. O. & Saeed, T. Deposition and characterization of cadmium sulfide thin films by chemical bath deposition. *J. Cryst. Growth* **158**, 497–504 (1996). https://doi.org/10.1016/0022-0248(95)00467-X.

[125] Mane, R. S. & Lokhande, C. D. Chemical deposition method for metal chalcogenide thin films. *Mater.Chem.Phys.* **65**, 1-31 (2000). https://doi.org/10.1016/S0254-0584(00)00217-0.

[126] Chu, T. L., Chu, S. S., Ferekides, C., Wu, C. Q., Britt, J. & Wang, C. 13.4% efficient thin-film CdS/CdTe solar cells. *J. Appl. Phys.* **70**, 7608-7612 (1991). https://doi.org/ 10.1063/1.349717.

[127] Hodes, G., Yaron, A. A., Decker, F. & Motisuke, P. Three-dimensional quantum-size effect in chemically deposited cadmium selenide films. *Phys. Rev. B* **36**, 4215-4221 (1987). https://doi.org/10.1103/physrevb.36.4215.

[128] Nemec, P., Nemec, I., Nahalkova, P., Nemcova, Y., Rojaneka, F. T. & Maly, P. Ammonia-free method for preparation of CdS nanocrystalline films by chemical bath deposition technique. *Thin Solid Films* 403–404, 9–12 (2002). https://doi.org/10.1016/S0040-6090(01)01530-9.

[129] Moncada, I. C., Gonzalez, L. A., Rodriguez-Galicia, J. L. & Rendon-Angeles, J. C. Chemical deposition of CdS films by an ammonia-free process with amino acids as complexing agents. *Thin Solid Films* 599, 166–173 (2016). https://doi.org/10.1016/j.tsf.2015.12.040.

[130] Lilhare, D., Pillai, S. & Khare, A. Effect of Tb Doping on structural and optical properties of ($Cd_{0.8}$-$Zn_{0.2}$)S films deposited through a chemical route. *J. Electron. Mater.* **47**, 6532-6539 (2018). https://doi.org/10.1007/s11664-018-6554-5.

[131] Komaki, H., Yamada, A., Sakurai, K., Ishizuka, S., Kamikawa-Shimizu, Y., Matsubara, K., Shibata, H. & Niki, S. CIGS solar cell with CdS buffer layer deposited by ammonia-free process. *Phys. Status Solidi A* 206, 1072–1075 (2009). https://doi.org/10.1002/pssa.200881159.

[132] Hariskos, D., Powalla, M., Chevaldonnet, N., Lincot, D., Schindler, A. & Dimmler, B. Chemical bath deposition of CdS buffer layer: prospects of increasing materials yield and reducing waste. *Thin Solid Films* **387**, 179–181 (2001). https://doi.org/10.1016/S0040-6090(00)01705-3.

[133] Malinowska, B., Rakib, M. & Durand, G. Cadmium recovery and recycling from chemical bath deposition of CdS thin layers. *Prog. Photovolt. Res. Appl.* **10**, 215–228 (2002). https://doi.org/10.1002/pip.402.

[134] Ortuno-Lopez, M. B., Sotelo-Lerma, M., Mendoza-Galvan, A., & Ramirez-Bon, R. Chemically deposited CdS films in an ammonia-free cadmium-sodium citrate system. *Thin Solid Films* **457**, 278–284 (2004). https://doi.org/10.1016/j.tsf.2003.11.169.

[135] Landin, R. O., Hernandez, J. S., Vigil, G. O. & Ramirez-Bon, R. Chemically deposited CdS by an ammonia-free process for solar cells window layers. *Sol. Energy* **84**, 208–214 (2010). https://doi.org/10.1016/j.solener.2009.11.001.

[136] Khallaf, H., Oladeji, I. O., Chai, G. & Chow, L. Optimization of chemical bath deposited CdS thin films using nitrilotriacetic acid as a complexing agent. *Thin Solid Films* **516**, 5967–5973 (2008). https://doi.org/10.1016/j.tsf.2007.10.079.

[137] Samadi-Maybodi, A., Abbasi, F. & Akhoondi, R. Aqueous synthesis and characterization of CdS quantum dots capped with some amino acids and investigations of their photocatalytic activities. *Colloids Surf. A*, **447**, 111–119 (2014). https://doi.org/10.1016/j.colsurfa.2014.01.036.

[138] Talwatkar, S. S., Tamgadge, Y. S., Sunatkari, A. L., Gambhire, A. B. & Muley, G. G. Amino acids (l-arginine and l-alanine) passivated CdS nanoparticles: Synthesis of spherical hierarchical structure and nonlinear optical properties. *Solid State Sci.* **38**, 42–48 (2014). https://doi.org/10.1016/j.solidstatesciences.2014.09.014.

[139] Mendivil-Reynoso, T., Berman-Mendoza, D., González, L. A., Castillo, S. J., Apolinar- Iribe, A., Gnade, B. Quevedo-López, M. A. & Ramirez-Bon, R. Fabrication and electrical characteristics of TFTs based on chemically deposited CdS films, using glycine as a complexing agent. *Semicond. Sci. Technol.* **26**, 115010 (2011). https://doi.org/10.1088/0268-1242/26/11/115010.

[140] Ferra-Gonzalez, S. R., Berman-Mendoza, D., Garcia-Gutierrez, R., Castillo, S. J., Ramirez-Bon, R., Gnade, B. E. & Quevedo-López, M. A. Optical and structural properties of CdS thin films grown by chemical bath deposition doped with Ag by ion exchange. *Optik* **125** 1533–1536 (2014). https://doi.org/10.1016/j.ijleo.2013.08.035.

[141] Carreon-Moncada, I., Gonzalez, L.A., Rodriguez-Galicia, J. L. & Rendon-Angeles, J. C. Chemical deposition of CdS films by an ammonia-free process with amino acids as complexing agents, *Thin Solid Films* **599**, 166–173 (2016). https://doi.org/10.1016/j.tsf.2015.12.040.

[142] Ortuno-Lopez, M. B., Valenzuela-Jauregui, J. J., Sotelo-Lerma, M., Mendoza- Galvan, A. & Ramırez-Bon, R. Highly oriented CdS films deposited by an ammonia-free chemical bath method. *Thin Solid Films* **429**, 34–39, (2003). https://doi.org/10.1016/S0040-6090(03)00144-5.

[143] Ortuno-Lopez, M. B., Sotelo-Lerma, M., Mendoza- Galvan, A. & Ramırez-Bon, R. Chemically deposited CdS films in an ammonia-free cadmium–sodium citrate system. *Thin Solid Films* **457**, 278–284 (2004). https://doi.org/10.1016/j.tsf.2003.11.169.

[144] Sandoval-Paz, M. G., Sotelo-Lerma, M., Mendoza-Galvan, A. & Ramırez- Bon, R. Optical properties and layer microstructure of CdS films obtained from an ammonia-free chemical bath deposition process. *Thin Solid Films* **515**, 3356–3362 (2007). https://doi.org/10.1016/j.tsf.2006.09.024.

[145] Sandoval-Paz, M. G., & Ramırez- Bon, R. Analysis of the early growth mechanisms during the chemical deposition of CdS thin films by spectroscopic ellipsometry. *Thin Solid Films* **517**, 6747–6752 (2009). https://doi.org/10.1016/j.tsf.2009.05.045.

[146] Ortuno-Lopez, M. B., Sotelo-Lerma, M., Mendoza-Galvan, A. & Ramirez- Bon, R. Optical band gap tuning and study of strain in CdS thin films. *Vacuum* **76**, 181–184 (2004). https://doi.org/10.1016/j.vacuum.2004.07.038.

[147] Hernandez-Borja, J., Vorobiev, Y. V. & Ramırez-Bon, R. Thin film solar cells of CdS/PbS chemically deposited by an ammonia-free process. *Sol. Energy Mater. Sol. Cells* **95**, 1882–1888 (2011). https://doi.org/10.1016/j.solmat.2011.02.012.

[148] Esparza-Ponce, H. E., Hernandez-Borja, J., Reyes-Rojas, A., Cervantes-Sanchez, M., Vorobiev, Y. V., Ramırez-Bon, R., Perez-Robles, J. F. & Gonzalez-Hernandez, J. Growth technology, X-ray and optical properties of CdSe thin films. *Mater. Chem. Phys.* **113**, 824–828 (2009). https://doi.org/10.1016/j.matchemphys.2008.08.060.

[149] Salas-Villasenor, A. L., Mejıa, I., Hovarth, J., Alshareef, H. N., K.Cha, D., Ramırez Bon, R., Gnade, B. E. & Quevedo-Lopez, M. A. Impact of gate dielectric in carrier mobility in low temperature chalcogenide thin film transistors for flexible electronics. *Electrochemical and Solid State Lett.* **13**, H313–H316 (2010). https://doi.org/10.1149/1.3456551.

[150] Arreola-Jardon, G., Gonzalez, L. A., Garcia-Cerda L. A., Gnade B., Quevedo- Lopez M. A. & Ramirez-Bon R. Ammonia-free chemically deposited CdS films as active layers in thin film transistors. *Thin Solid Films* **519**, 517–520 (2010). https://doi.org/10.1016/j.tsf.2010.08.097.

[151] Watanabe, S. & Mita, Y. Electrical properties of CdS/PbS heterojunctions. *Solid State Electron.* **15**, 5–10 (1972). https://doi.org/10.1016/0038-1101(72)90061-5.

[152] Elabd, H. & Steckl, A. J. Auger analysis of the PbS-Si heterojunction. *J. Electron. Mater.* 9, 525–549 (1980).

[153] Ellingson, R. J., Beard, M. C., Johnson, J. C., Yu, P., Micic, O. I., Nozik, A. J., Shabaev, A. & Efros, A. L. Highly efficient multiple exciton generation in colloidal PbSe and PbS quantum dots. *Nano Lett.* **5**, 865–871 (2005). https://doi.org/10.1021/nl0502672.

[154] Perna, G., Capozzi, V., Ambrico, M., Augelli, V., Ligonzo T., Minafra A., Schiavulli L. & Pallara M. Structural and optical characterization of undoped and indium-doped CdS films grown by pulsed laser deposition. *Thin Solid Films* **453–454**, 187-194 (2004). https://doi.org/10.1016/j.tsf.2003.11.105.

[155] Opanasyuk, A. S., Kurbatov, D. I., Ivashchenko, M. M. & Protsenko, I. Y. Properties of the window layers for the CZTSe and CZTS based solar cells. *J. Nano Electron. Phys.* **4**, 01024-1-01024-3 (2012).

[156] Han, J., Liao, C., Jiang, T., Spanheimer, C., Haind, G., Fu, G., Krishnakumar, V., Zhao, K., Klein, A. & Jaegermann, W. An optimized multilayer structure of CdS layer for CdTe solar cells application,. *J. Alloys Compd.* **509**, 5285-5289 (2011). https://doi.org/10.1016/j.jallcom.2010.12.085.

[157] Xu X., Wang, X., Gu, W., Quan, S. & Zhang, Z. Study on influences of CdZnS buffer layer on CdTe solar cells. *Superlattices Microstruct.* **109**, 463-469 (2017). https://doi.org/10.1016/j.spmi.2017.05.033.

[158] Pudov, A., Sites, J. & Nakada, T. Performance and loss analyses of high-efficiency chemical bath deposition (CBD) ZnS/Cu($In_{1-x}Ga_x$)Se_2 thin-film solar cells. *Jpn. J. Appl. Phys.* **41**, L672-L674 (2002). https://doi.org/10.1143/JJAP.41.L672.

[159] Yang, L. C., Xiao, H. Z., Rockett, A., Shafarman, W. N. & Birkmire, R. W. The growth by the hybrid sputtering and evaporation method and microstructural studies of $CuInSe_2$ films. *Sol Energy Mater Sol Cells* **36**, 445-455 (1995). https://doi.org/10.1016/0927-0248(94)00192-8.

[160] Mohamed, H. A. Dependence of efficiency of thin-film CdS/CdTe solar cell on optical and recombination losses. *J. Appl. Phys.* **113**, 093105 (2013). https://doi.org/10.1063/1.4794201.

[161] Kumar, S. G. & Koteshwara Rao, K. S. R. Physics and chemistry of CdTe/CdS thin film heterojunction photovoltaic devices: fundamental and critical aspects. *Energy Environ. Sci.* **7**, 45-102 (2014). https://doi.org/10.1039/C3EE41981A.

[162] Da Cunha, A. F., Kurdesau, F. & Salome, P. M. P. Performance comparison of hybrid sputtering/evaporation $CuIn_{1-x}Ga_xSe_2$ solar cells with different transparent conducting oxide window layers. *J. Non-Cryst. Solids* 352, 1976-1980 (2006). https://doi.org/10.1016/j.jnoncrysol.2005.12.028.

[163] Fujiwara, H. *Spectroscopic Ellipsometry Principles and Applications*. John Wiley & Sons Ltd. UK (2007).

[164] Hossain, M. S., Rahman, K. S., Karim, M. R., Aijaz, M. O., Dar, M. A., Shar, M. A., Misran, H., Amin, N., Impact of CdTe thin film thickness in $Zn_xCd_{1-x}S$/CdTe solar cell by RF sputtering, *Sol. Energy* **180**, 559-566 (2019). https://doi.org/10.1016/j.solener.2019.01.019.

[165] Kasim, U., Narayanan, H., Anthony, O., Optimization of Process Parameters of Chemical Bath Deposition of $Cd_{1-X}Zn_xS$ Thin Film, *Leonardo J. Sci.* **12**, 111-120 (2008).

[166] Kartopu, G., Clayton, A. J., Brooks, W. S. M., Hodgson, S. D., Barrioz, V., Maertens, A., Lamb, D. A., Irvine, S. J. C., *Prog. Photovolt: Res. Appl.* (2012). https://doi.org/10.1002/pip.2272.

[167] Brooks, W. S. M., Irvine, S. J. C., Barrioz, V., Clayton, A. J., Laser beam induced current measurements of Cd1−xZnxS/CdTe solar cells, *Sol. Energy Mater. Sol. Cells* **101**, 26–31 (2012). https://doi.org/10.1016/j.solmat.2012.02.006.

[168] Castillo, R. H., Acosta, M., Riech, I., Rodriguez, G. S., Gamboa, J. M., Acosta C., Zambrano, M., Study of ZnS/CdS structures for solar cells applications, *Optik* 148, 95–100 (2017). https://doi.org/10.1016/j.ijleo.2017.09.002.

[169] Osman, M. A. & Abd-Elrahim, A. G. Excitation wavelength dependent photoluminescence emission behavior, UV induced photoluminescence enhancement and optical gap tuning of $Zn_{0.45}Cd_{0.55}S$ nanoparticles for optoelectronic applications. *Optical Mater.* **77**, 1–12 (2018). https://doi.org/10.1016/j.optmat.2018.01.011.

[170] Osman, M. A., Abd-Elrahim, A. G. & Othman, A. A. Size-dependent structural phase transitions and their correlation with photoluminescence and optical absorption behavior of annealed $Zn_{0.45}Cd_{0.55}S$ quantum dots. *Mater. Character.* **144**, 247–263 (2018). https://doi.org/10.1016/j.matchar.2018.07.020.

[171] Prem Kumar, T. & Sankaranarayanan K. Tunability of structural, surface texture, compositional and optical properties of CdZnS thin films by photo assisted-chemical bath deposition technique. *Chalcogenide Lett.* **6**, 617–622 (2009).

[172] Werta, S. Z., Echendu, O. K., Egbo, K. O. & Dejene F. B. Electrochemical deposition and characterization of thin-flm $Cd_{1-x}Zn_xS$ for solar cell application: The effect of cathodic deposition voltage. *Thin Solid Films* **689**, 137511 (2019). https://doi.org/10.1016/j.tsf.2019.137511.